Interval Timing Under a Behavioral Microscope: Dissociating Motivational and Timing Processes in Fixed-Interval Performance

by

Carter W. Daniels

A Thesis Presented in Partial Fulfillment
of the Requirements for the Degree
Master of Arts

Approved November 2015 by the
Graduate Supervisory Committee:

Federico Sanabria, Chair
Clive Wynne
Gene Brewer

ARIZONA STATE UNIVERSITY

December 2015

ABSTRACT

Theories of interval timing have largely focused on accounting for the aggregate properties of behavior engendered by periodic reinforcement, such as sigmoidal psychophysical functions and their scalar property. Many theories of timing also stipulate that timing and motivation are inseparable processes. Such a claim is challenged by fluctuations in and out of states of schedule control, making it unclear whether motivation directly affects states related to timing. The present paper seeks to advance our understanding of timing performance by analyzing and comparing the distribution of latencies and inter-response times (IRTs) of rats in two fixed-interval (FI) schedules of food reinforcement (FI 30-s and FI 90-s), and in two levels of food deprivation. Computational modeling revealed that each component was well described by mixture probability distributions embodying two-state Markov chains. Analysis of these models revealed that only a subset of latencies are sensitive to the periodicity of reinforcement, and pre-feeding only reduces the size of this subset. The distribution of IRTs suggests that behavior in FI schedules is organized in bouts that lengthen and ramp up in frequency with proximity to reinforcement. Pre-feeding slowed down the lengthening of bouts and increased the time between bouts. When concatenated, these models adequately reproduced sigmoidal FI response functions. These findings suggest that behavior in FI fluctuates in and out of schedule control; an account of such fluctuation suggests that timing and motivation are dissociable components of FI performance. These mixture-distribution models also provide novel insights on the motivational, associative, and timing processes expressed in FI performance, which need to be accounted for by causal theories of interval timing.

DEDICATION

I would like to dedicate this work to my family, friends, and committee all of whom have had to suffer way too many discussions on the intricacies of psychology and the philosophy of science. In particular, my mother, Katherine Daniels for supporting me in my desire to focus on something other than engineering and Jennifer Laude for always letting me think out loud about whatever I happen to be working on at the time and her constant support in my endeavors. Dr. Federico Sanabria for helping me to turn my ideas into concrete experiments and opening my mind to the world that is mathematical modeling. Dr. Gene Brewer and Dr. Clive Wynne for their encouragement and discussions pertaining to this project and the future. Dr. Peter Killeen for his support and discussions concerning research. Also my old lab mates, Dr. Elizabeth Watterson, Dr. Gabriel Mazur, and Dr. Ryan Brackney for their comradery through my first two years in graduate school. Finally, I dedicate this work, and all other work I do to my grandfather, Robert Lillon Carter, who always provided helpful guidance and support throughout his life.

ACKNOWLEDGMENTS

This research was supported by the National Institutes of Health (MH094562), a seed grant from the College of Liberal Arts and Sciences, Arizona State University, and a Grant-in-Aid of Research from the National Academy of Sciences, administered by Sigma Xi, The Scientific Research Society. I would like to thank Raul Garcia, Paula Overby, Christine Herrera, Jesse St. Amand, Sanjana Khana, Natasha Sinchuk, and Jake Gilmour, Briana Martinez, Andrew Nye, and Cavan Winikates for helping with data collection.

TABLE OF CONTENTS

Page

CHAPTER Page

LIST OF TABLES

LIST OF FIGURES

CHAPTER 1

INTRODUCTION

Interval timing is the entrainment of an animal's behavior to a target periodicity in the environment, on the basis of an endogenous time-keeping mechanism (Buhusi & Meck, 2005; Oprisan & Buhusi, 2011). This process is often studied using fixed interval (FI) schedules of reinforcement. In FI schedules, the first response after some interval has elapsed is reinforced. The behavior engendered by FI schedules is highly regular: following an initial pause, or *latency*, mean response rate increases and plateaus near the end of the interval. This organization of behavior has been observed in a wide range of species (Lejeune & Wearden, 1991) and also in Pavlovian conditioning. Indeed, Pavlov observed that, in the presence of a temporally extended conditioned stimulus, well-trained animals initially pause before responding continually until the expected time of reinforcement (Pavlov, 1927; Rescorla, 1967; Vogel, Brandon, & Wagner, 2003). The resemblance between FI performance and performance in Pavlovian analogues has stimulated much theory development (Kalafut, Freestone, MacInnis, & Church, 2014; Molet & Miller, 2014; Harris, 2015).

The foundation of many theories of timing is a basic computational structure first formalized by Treisman (1963). Briefly, onset of a stimulus, signaling the to-be-timed interval, empties an accumulator and initiates the emission of pulses from a pacemaker to the accumulator (together, these comprise the *internal clock*). Once the pulse count in the accumulator becomes similar to a pulse count criterion sampled from memory, a target response (e.g., reporting that 10 s have elapsed) is emitted. Following reinforcement, pulses in the accumulator update memory. This simple structure yields a temporal

distribution of the target response centered on a proportion of the to-be-timed interval (see Appendix A of Daniels, Watterson, Garcia, Mazur, Brackney, & Sanabria, 2015 for a mathematical description of this mechanism).

Theories of timing typically differ in how they instantiate the components of the timing mechanism. For instance, the behavioral theory of timing suggests that transitions between behavioral states constitute pulses (Killeen & Fetterman, 1988; Machado 1997), whereas the multiple timescales theory of timing suggests that the clock is a form of memory decay (Staddon, 2005; Staddon, Chelaru, & Higa, 2002; Staddon & Higa, 1999). More recently, theorists have attempted to ground the basic mechanism into biologically plausible neural networks (Oprisan & Buhusi, 2011; Karmarkar & Buonomano, 2007) and in drift diffusion models that appear to approximate neuron dynamics (e.g. Simen, Rivest, Ludvig, Balci, & Killeen, 2013; Simen, Balci, deSouza, Cohen, & Holmes, 2011). The challenge for these theories is to account for a variety of classic properties of interval timing. In the context of FI schedules, this includes the sigmoidal response function and the scalar property (Guilhardi & Church, 2005; Machado, Malheiro, & Erlhagen, 2009). However, these aggregate properties of behavior provide a relatively weak criterion for selecting among models of timing, because most of these models, despite their widely different assumptions, provide a reasonable account of such properties. Other properties of timing performance, such as its responsiveness to motivational manipulations, may provide more informative criteria for selecting between models of timing.

Accounting for the effect of motivational manipulations on timing performance involves some substantial challenges. Recent studies suggest that timing and motivation processes are intimately related (Avlar, Kahn, Jensen, Kandel, Simpson, Balsam, 2015;

Balci, 2014; Kirkpatrick, 2013). Consistent with this with relation, neural circuits implicated in interval timing also regulate incentive motivation processes (Berridge & Kringlebach, 2013; Kirkpatrick, 2013; Coull, Hwang, Leyton, & Dagher, 2012). However, such conclusions are often drawn from theoretical frameworks that assume, while in a timing task, subjects are always engaged in timing. Such an assumption is inconsistent with the hypothesis that responsiveness to the temporal regularities of periodic stimuli fluctuates between trials (Daniels et al., 2015a,b; Freestone, Balci, Simen, & Church, 2014; Mazur, Wood-Isenberg, Watterson, & Sanabria, 2014; Mika, Mazur, Goffman, Talboom, Bimonte-Nelson, Sanabria, & Conrad, 2012; Sanabria & Killeen, 2008; Lejeune & Wearden, 1991). This hypothesis suggests, at the beginning of each trial, subjects enter either a timing-state and emit target responses generated by a timing mechanism, or they enter a non-timing state and emit target responses randomly. Furthermore, fluctuation in timing performance may reflect a more general fluctuation in behavioral control by operant schedules (Cheung, Neisewander, & Sanabria, 2012; Brackney, Cheung, Neisewander, & Sanabria, 2011; Shull 2004; Shull, Grimes, & Bennet, 2004; Shull, Gaynor, & Grimes, 2001, 2002; Gibbon, 1995; Meyerson & Miezen, 1980).

Timing performance, as engendered by FI schedules, is thus likely a composite of multiple two-state processes that animals cycle into and out of until reinforcement is obtained. Although previous studies have attempted to implement models embodying this notion (Harris, 2015; Guilhardi and Church, 2005; Kirkpatrick, 2002), it remains poorly characterized in the context of FI and have yet to be fully appreciated. Validation and implementation of fluctuation models in the analysis of FI performance would provide

clarity on whether or not timing and motivation are related (Balci, 2014; Kirkpatrick, 2014; Galtress, Marshall, & Kirkpatrick, 2012; Ludvig, Balci, & Spetch, 2011; Balci et al., 2010; Galtress & Kirkpatrick, 2010; Sanabria, Thrailkill, & Killeen, 2009; Belke & Christie-Fougere, 2006; Ludvig, Conover, & Shizgal, 2007; Plowright, Church, Behnke, & Silverman, 2000). Specifically, if motivation and timing are inseparable, manipulations of motivation should influence performance in the timing state; if motivation and timing are dissociable, manipulations of motivation should influence performance only in the non-timing state. The latter finding would reinforce the notion that timing is robust to changes in the motivational state of the animal (Gibbon, 1977; Gibbon, 1995).

Thus, the purpose of the present study was two-fold: (1) to isolate the potential stochastic processes underlying FI performance by determining whether individual components of FI performance are best described by two-state models, and (2) to determine which of those processes are affected by motivational manipulations. Using strategies formulated by Killeen, Hall, Reilly, & Kettle (2002), the present study pursued these goals by conducting a microstructural analysis of performance (Cheung et al., 2012) in two FI schedules and two levels of food deprivation.

Fig. 1 shows a schematic of how behavior is organized in an FI trial. In a well-trained animal, performance in an FI trial begins with a latency, followed by responses of various durations (RDs) that alternate with inter-response times (IRTs). A theoretically-motivated generative model of latencies and IRTs was derived from a general model of operant performance (Brackney et al., 2011). For RDs, the empirical data were leveraged to help recover aggregate performance. According to this general model, underlying each component is a two-state process wherein the animal either enters a schedule-controlled

state (latencies are timed, IRTs are short) or it enters an alternative state (latencies of random length, IRTs are long). The analysis also determined the extent to which the parameters that generate IRTs change as a function of time in the FI.

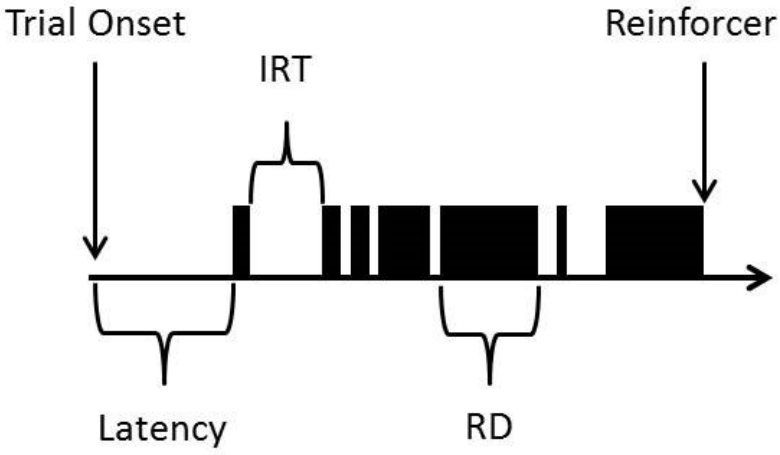

Fig. 1. Illustrative diagram of FI responding in a fixed-interval (FI) trial. Performance begins with a latency and is followed by a series of responses (black bars) of variable duration (RD) separated by inter-response times (IRTs). RDs and IRTs repeat until the reinforcer is delivered following a response.

For two groups of food-deprived rats, head-entries into a food receptacle were reinforced according to a FI 30-s (group FI30) or a FI 90-s (group FI90) schedule, until performance stabilized according to a pre-defined criterion. FI90 rats were then exposed to a pre-feeding manipulation for 5 sessions. Following data collection, a model-space investigation was conducted to determine whether the full complexity of a two-state static or dynamic model was justified to describe each component of performance. Then, the effects of schedule and pre-feeding manipulations on parameter estimates were assessed. Finally, a simulation of FI performance based on parameter estimates was conducted to recover the empirical response functions.

CHAPTER 2

METHODS

Subjects

Sixteen male Wistar rats (Charles River Laboratories, Hollister, CA), divided into 2 cohorts (groups FI30 and FI90), served as subjects. Rats arrived on post-natal day 60 and were pair-housed immediately upon arrival. Rats were housed on a 12:12 h light cycle, with dawn at 1900 h; all behavioral training was conducted during the dark phase of the light cycle. Behavioral training and food restriction protocols were implemented shortly after arrival. Access to food was reduced daily from 24, to 18, 12, and finally 1 h/day. During behavioral training, food was provided 30 min after the end of each training session, such that at the beginning of the next session weights were, on average, 85% of mean ad libitum weights estimated from growth charts provided by the breeder. Water was always available in home cages. All animal handling procedures followed National Institutes for Health guidelines and were approved by the Arizona State University Institutional Animal Care and Use Committee.

Apparatus

Experiments were conducted in 8 MED associates (St. Albans, VT, USA) modular test chambers (305 mm long, 241 mm wide, and 210 mm high), each enclosed in a sound- and light-attenuating box equipped with a ventilation fan that provided masking noise of approximately 60 dB. The front and back walls and the ceiling of test chambers were made of Plexiglas; the front wall was hinged and served as a door to the chamber. The floor consisted of thin metal bars positioned above a catch pan. One of the two aluminum side panels served as a test panel. The reinforcer receptacle was a square

opening (51-mm sides) located 15 mm above the floor and centered on the test panel. The receptacle provided access to a dipper (MED Associates, ENV-202M-S) fitted with a cup (ENV-202C) that could hold 0.01 cc of a liquid reinforcer (33% sweetened condensed milk diluted in tap water; Great Value brand, Walmart, Bentonville, AK). The receptacle was furnished with a head-entry detector (ENV-254-CB). A house-light located behind the wall opposite to the test panel could dimly illuminate the test chamber. Experimental events were arranged via a MED PC® interface connected to a PC controlled by MED-PC IV® software.

Procedure

All training sessions for each group were conducted once daily, 7 days/week.

Phase 1: chamber and reinforcer acclimation. Each session began with a 3-min warm-up period during which the house-light was on. After completion of this warm-up period, each trial began by turning off the house-light. Reinforcement was programmed according to a fixed-time (FT) 30-s schedule of reinforcement for group FI30 and a FT 90-s schedule of reinforcement for group FI90. The end of the interval was followed by a 5-s reinforcer and onset of the house-light, which was on until the completion of the inter-trial interval (ITI). The ITI was in effect until the rat removed its head from the reinforcement receptacle for 2 s. For FI30 and FI90 rats each session lasted 60 and 180 min, respectively, or until 60 reinforcers were earned. Although the duration of sessions for each group was different, it ensured a similar number of trials per session. The number of head-entries into the reinforcement receptacle during every FT interval was measured; all rats had to make 30 or more head-entries in a session to progress to the next phase. This phase lasted 5 sessions.

Phase 2: FI training. FI-training sessions were similar to those in phase 1, but reinforcement was delivered only if (a) the rat's head was detected inside the reinforcer receptacle, and (b) the FT had elapsed; reinforcement was therefore programmed on a fixed-interval (FI) 30-s schedule for group FI30 and a FI 90-s schedule for group FI90. Training continued for a minimum of 20 sessions and until all rats demonstrated stable temporal control. Stability was determined by a non-significant ($p > .05$) regression of the median and inter-quartile range (IQR) of latencies (the interval between trial onset and first head-entry) over 5 consecutive sessions. FI30 rats were trained for 23 sessions; FI90 rats were trained for 25 sessions.

Phase 3: pre-feeding. Sessions were similar to those in phase 2, except that the daily 1 h of free access to food in the home cage was provided immediately prior to the session instead of 30 min after the session. This phase was implemented for 5 sessions. Only rats in group FI 90 were exposed to this phase.

Data Analysis

During phases 2 and 3, the time of occurrence and duration of every head-entry into the reinforcement receptacle was measured in every trial, except for the first trial in each session which was considered a warm-up trial. Data from the last 5 sessions of phase 2 served as steady-state baseline performance for groups FI30 and FI90; data from the 5 sessions of phase 3 served as pre-feeding performance for group FI90. For each baseline and pre-feeding trial, each component of FI responding—latency, inter-response times (IRTs), and response durations (RDs)—was obtained.

Latencies and IRTs were modeled and quantitatively analyzed on the basis of well-specified theories of timing and operant behavior. Because no such theory is

available for RDs, these were not modeled and were only qualitatively analyzed. Latencies and IRTs were fit to variations of a shifted gamma-exponential mixture distribution,

$$\begin{aligned} &p(x_t < \delta) = 0, \\ &p(x_t \geq \delta) = q_t \Gamma(x_t - \delta; 1 + \varepsilon_t, c_t) + (1 - q_t)\exp(x_t - \delta; k_t) \end{aligned} \quad . \qquad 1 \geq q_t \geq 0; \varepsilon_t, c_t, k_t \geq 0 \quad (1)$$

In Eq. 1, the probability of a latency or of an IRT sampled at time t in the interval (0-30 s in FI30, 0-90 s in FI90) is the weighted average of a gamma distribution Γ with shape and scale parameters $1 + \varepsilon_t$ and c_t, respectively, and an exponential distribution with mean and standard deviation k_t. Eq. 1 is a model of timing performance, in which temporal judgments are gamma distributed and random non-timing durations are exponentially distributed (Daniels et al., 2015a,b; Mazur et al., 2014; Sanabria & Killeen, 2008). Parameter δ is the shortest data observed and not a free parameter; it is intended to capture the minimum amount of time necessary emit a response and thus reflects motoric capacity (Cheung et al., 2012; Brackney et al., 2011; Killeen & Sitomer, 2003; Killeen, 1994). Note that Γ reduces to an exponential distribution when $\varepsilon_t = 0$; under such constraint, Eq. 1 describes the distribution of IRTs when responses are organized in bouts. Such organization accounts for operant-level behavior (Cabrera, Sanabria, Jimenez, & Covarrubias, 2013), adjunctive behavior (Ibias, Sanabria, & Pellon, 2015), visit times in concurrent variable-interval (VI) schedules of reinforcement (Gibbon, 1995), and performance under single VI schedules of reinforcement (Brackney et al., 2011; Hill, Herbst, & Sanabria 2012; Fulton, Conover, & Shizgall, 2001).

By definition, latencies are always sampled at the beginning of each trial, so $t = 0$. However, IRTs may change as a function of t, yielding the typical sigmoidal-shaped

function of response rate over the interval. To account for these potential changes, it was assumed that (a) the parameters of the gamma and exponential distributions and the odds against sampling from Γ, $J_t = (1 - q_t) / q_t$ could change exponentially over the interval, and such change (b) may not begin until some interval τ has elapsed, and (c) asymptotes at Ω. Expressed as equations,

$$\left.\begin{aligned} J_t &= J_0 \\ c_t &= c_0 \\ k_t &= k_0 \end{aligned}\right\} \quad if\ \tau \le t\,,$$

$$\left.\begin{aligned} J_t &= J_0 e^{\gamma(t-\tau)} \\ c_t &= (c_0 - \Omega)e^{\alpha(t-\tau)} + \Omega \\ k_t &= (k_0 - \Omega)e^{\beta(t-\tau)} + \Omega \end{aligned}\right\} \quad if\ \tau > t\,, \qquad J_0, c_0, k_0, \tau, \Omega \ge 0 \quad (2)$$

where γ, α, and β are the change parameters of J_t, c_t, and k_t, respectively. As mentioned before, for IRTs ε = 0 and invariant, and thus no decay parameter is specified. Eq. 2 is a general model of change in operant IRTs, so no direction of change is assumed (i.e., change rates may be positive or negative), because the direction of change may vary depending on the schedule of reinforcement (e.g., negative in FI, but positive in extinction).

To distinguish between models, latency and IRT parameters are subscripted with *L* and *I*, respectively; for example, for IRTs, c_{It} is the scale parameter of Γ at time *t*. Taken together, Eqs. 1-2 comprise a general model from which the models of each component of FI performance are special cases. For latencies, *t* = 0, and thus γ, β, τ, and Ω are indeterminate. Additionally, for latencies, δ = 0 because, otherwise, it would imply that the actual interval being timed is equal to FI – δ instead of the FI. Responses post latency were expected to be organized in bouts emitted at random times, thus IRTs were

expected to be distributed such that $\varepsilon_{I0} = 0$ and, to provide meaning to q, $k_{It} > c_{It}$. In the absence of a theory of RDs, the empirical distribution of RDs for each rat in each condition was used for posterior predictive checks of FI response functions.

The model of each component of FI performance, derived from the general model of operant performance described in Eq. 1-2, contains other nested models that correspond to different hypotheses about the distribution underlying each component. For example, in the case of latencies, the nested model where $q_{L0} = 1$ corresponds to the hypothesis that all latencies are gamma distributed. The motivation for each nested model and its corresponding component of FI performance is detailed in their corresponding sections; they were validated using the method of maximum likelihood (Myung, 2003) and the corrected Akaike Information Criterion (AICc; Burnham & Anderson, 2002). AICc is a model selection criterion that favors models that balance high likelihood with low complexity. See Appendix A for further details concerning the model selection process.

Selected models were fit to the baseline data of each rat in groups FI30 and FI90 and to the pre-feeding data of each rat in group FI90. Parameter estimates and derived statistics were log transformed or, in the case of q, log-odds transformed for statistical analysis (Cheung et al., 2012). The MLE method sometimes yields extreme estimates when applied to mixture-distribution models (Cheung et al., 2012). Thus, prior to each statistical analysis a two-tailed Grubbs' test was performed on log-transformed estimates to detect potential outliers. Outlier data was removed when it was detected with $\alpha = .05$; in most instances, outliers were detected with $\alpha = .01$ and removal of the outlier did not change whether or not a statistical test was significant. Statistical analysis consisted of

independent t-tests or Welch's t-test (in the case of unequal ns due to removal of an outlier) of the effect of FI schedule (baseline FI30 vs. FI90), and dependent t-tests of the effect of pre-feeding (baseline FI90 vs. pre-feeding FI90), with $\alpha = .05$. All parameter estimates are reported back-transformed ±SEM.

CHAPTER 3

RESULTS

The top panel of Fig. 2 shows the mean probability of a response as a function of time in the FI 30-s and FI 90-s schedules. Baseline behavior appears to be under temporal control of the schedule for rats in groups FI30 and FI90, as suggested by the progressive increase in response probability, plateauing close to the end of interval. The mean probability of responding at the end of the interval was slightly higher in FI30 (.80) than in FI90 (.70).

The middle panel of Fig. 2 shows the data from the top panel on a normalized x-axis (time divided by FI duration) and y-axis (proportion of maximum probability of responding). During the first tenth of the interval, response probability rose more rapidly towards its maximum for FI90 than for FI30 rats. In the remainder of the interval, however, the relative steepness of these slopes was reversed, mostly because of changes in the slope of response probability in FI90 rats. This suggests strict adherence to Weber's law may not be observed.

The bottom panel of Fig. 2 shows the response probability function of baseline and pre-feeding FI 90-s performance. Pre-feeding appears to flatten the slope of the response probability function and shift it to the right.

Latencies

Model-space investigation. The top panel of Fig. 3 shows the mean empirical cumulative distribution of latencies for groups FI30 and FI90; the middle panel shows the same data normalized against the FI duration; the bottom panel shows group FI90 performance during baseline and pre-feeding conditions. Latencies for both groups

appear to be gamma-distributed, as predicted by some timing models (Killeen & Fetterman, 1988; Machado, 1997). Previous research suggests that only a portion of intervals produced in a timing task are sensitive to the passage of time (Daniels et al., 2015a,b; Mazur et al., 2014; Mika, et al, 2012; Sanabria & Killeen, 2008). This suggests an underlying two-state process wherein at the beginning of every trial the rat either enters a timing state with probability q_L or enters a non-timing state with probability 1 – q_L. When rats are in the timing state they emit latencies that are sensitive to the timing of reinforcement, and are thus gamma distributed. When rats are in the non-timing state they emit responses randomly with constant probability, thus yielding exponentially-distributed latencies. The resulting mixture distribution may be expressed as

$$p(x_L) = q_t\Gamma(x_L;1+\varepsilon_L,c_L) + (1-q_L)\exp(x_L;k_L); \qquad 1 \geq q_L \geq 0; \varepsilon_L, c_L, k_L \geq 0 \quad (3)$$

the meaning of each parameter of Eq. 3 is described in Table 1.

Table 1
Latency Distribution Parameters (Eq. 3)

Parameter	Unit	Meaning
q_L		Proportion of timed latencies.
$1+\varepsilon_L$	pulses	Number of pulses that must accumulate before emission of response.
c_L	s	Mean interval between pulses.
k_L	s	Mean non-timed latency

Note. Parameter q_L is a dimensionless proportion. The mean timed latency is $c_L\varepsilon_L$ and the standard deviation of timed latencies is $c_L\sqrt{(\varepsilon_L)}$.

The results of the model-space investigation are reported in Appendix B; fits to individual rats are visualized in Appendix C. Of the three models tested, allowing q_L to vary freely between 0 and 1 provided the best balance between fit and parsimony. The selected model was e^{110} times more likely than the next-best model, in which $q_L = 1$. Estimates of the parameters of the selected model are shown in Table 2. According to

these estimates, FI30 and FI90 rats entered a timing state, on average, on 80% of trials. When timing, rats produced gamma-distributed latencies of about 12 s and 45 s, for FI30 and FI90 respectively. When not timing, rats produced exponentially-distributed latencies of about 6 s and 17 s, for FI30 and FI90, respectively.

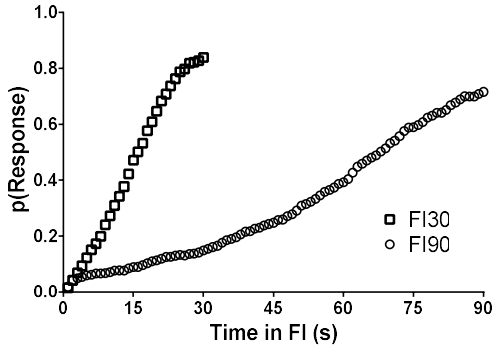

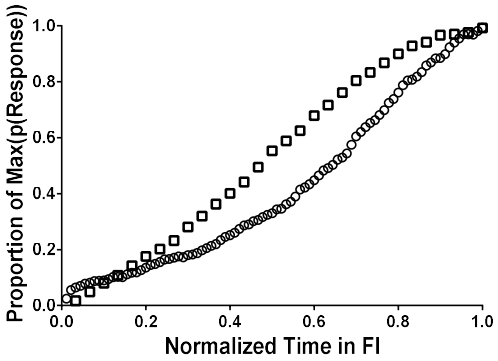

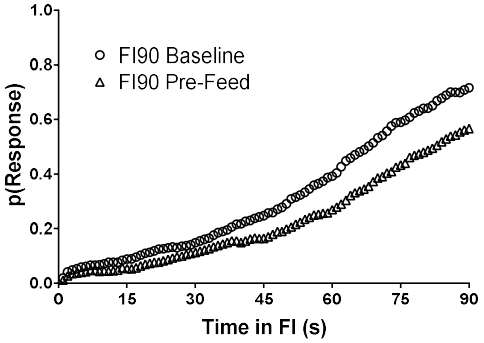

Fig. 2. Top Panel: Mean response function for group FI30 (squares) and FI90 (circles) as a function of time in the FI. The response function of each rat is the probability of detecting a head-entry as a function of time (in 1-s bins) in the FI. Middle Panel: Mean normalized response functions. Normalization was conducted for each rat by representing time as a proportion of the FI, and representing response probability as a proportion of the maximum response probability. Bottom Panel: Mean response function of FI90 baseline (circles) and pre-feeding (triangles) performance.

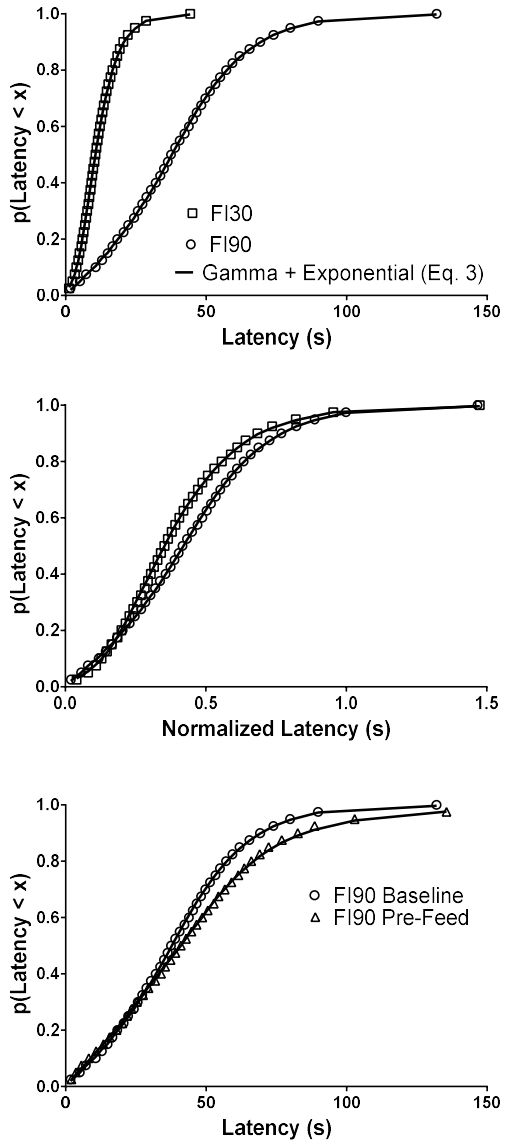

Fig. 3 Top Panel: Mean empirical cumulative distribution of latencies for groups FI30 (squares) and FI90 (circles). Middle Panel: Mean distribution of normalized latencies. Normalization was conducted for each rat by representing time as a proportion of the FI. Bottom Panel: Mean distribution of latencies for baseline FI90 (circles) and pre-feeding

(triangles) performance. Solid lines are mean traces of Eq. 3. Latencies are organized in 40 bins of equal number of latencies.

Table 2
Mean Parameter Estimates and Derived Statistics of the Distribution of Latencies

	FI 30		FI 90		FI 90 Pre-Feeding	
Parameter	*M*	*SEM*	*M*	*SEM*	*M*	*SEM*
q_L	0.818	0.061	0.776	0.039	0.574	0.091
$1+\varepsilon_L$ (pulses)	4.009	0.621	4.69	.549	9.137	2.527
c_L (s)	3.262 (.109)	0.408	8.633 (.096)	0.979 (.011)	7.718	1.149
k_L (s)	5.883 (.196)	1.979 (.066)	16.618 (.185)	4.525 (.050)	34.393	6.672
Derived Statistic						
Mean of Gamma (s)	12.231 (.407)	1.226 (.041)	45.422 (.505)	5.023 (.056)	54.659	7.744
SD of Gamma (s)	6.237 (.208)	0.613 (.020)	19.195 (.213)	1.305 (.015)	18.591	1.255
CV of Gamma	0.521	0.031	0.476	0.025	0.398	0.054
Mean Latency (s)	11.695 (.389)	1.264 (.042)	39.411 (.438)	4.449 (.049)	78.365	13.131

Note. Values in parentheses are non-parenthetical estimates divided by the corresponding FI. Derived statistics are computed from parameter estimates. CV is the coefficient of variation; CV = SD / mean. The means, SEM, and rescaled means and SEM do not contain outliers detected by Grubbs' test. The pulse count $1+\varepsilon_L$ is not rescaled because $CV = 1/\sqrt{(1+\varepsilon_L)}$, and thus rescaling $1+\varepsilon_L$ would constitute rescaling an already normalized value.

Schedule and pre-feeding effects on latencies. Grubbs' test revealed a single outlier for the estimation of ε_L and the derived coefficient of variation (CV), rat 2 in group FI30, $p < .05$, and was removed from statistical analysis. There were significant differences between FI30 and FI90 performance in estimates of c_L [$t(14) = 5.549$, $p < .001$] and k_L [$t(14) = 2.227$, $p = .043$], the mean and SD of the gamma distribution [$t(14) = 8.819$, $p < .001$; $t(14) = 10.131$, $p < .001$], and the mean latency predicted by the model

[t(14) = 7.809, $p < .001$]. These parameters and derived statistics appear to increase as duration of the FI schedule increases; all other tests were nonsignificant, all ps > .050.

Values in parentheses in Table 2 are the parameter estimates and derived statistics rescaled relative to the FI duration; the same outliers were detected as before. Independent t-tests revealed no significant differences in rescaled parameter estimates and derived statistics, all ps > .050 (see note about rescaling of $1+\varepsilon_L$ in Table 2). The absence of other significant effects suggests that all mean parameter estimates and derived statistics are approximately proportional to the duration of the FI. This is consistent with the absence of a significant difference in CV across FI schedules. Thus, it appears that both timed and non-timed latencies are scalar invariant. This is because timed-pulses and non-timed pulses appear to be emitted at intervals (c_L and k_L, respectively) proportional to those between trial onset and reinforcement.

Table 2 also shows the mean parameter estimates and derived statistics from Eq. 3 for FI90 pre-feeding performance. For all potential comparisons, Grubbs' test revealed a single outlier for the estimates of ε_L, c_L, q_L, and the derived mean and CV of the gamma distribution: rat 6 under pre-feeding; all ps < .05, and was removed from statistical analysis for those parameters. Pre-feeding significantly reduced q_L [t(6) = 3.498, p = .010], and increased k_L [t(7) = 2.675, p = .032] and the mean latency predicted by the model [t(7) = 3.501, p = .009]; all other tests were nonsignificant (all ps > .050). These results suggest that pre-feeding increases the prevalence and length of non-timed latencies.

Inter-Response Times

Model-space investigation. Previous research suggests that operant responses are organized in bouts separated by relatively long pauses (Smith, McLean, Shull, & Hughes, 2013; Cheung et al., 2012; Brackney et al., 2011; Shull, 2004; Shull et al., 2002, 2001; Fulton et al., 2002). Within-bout and between-bout responses are emitted randomly at a constant high (within-bout) or low (between-bout) rate. Inter-response times (IRTs) are thus distributed according to a mixture of two exponential distributions,

$$p(x_{It} < \delta_I) = 0,$$
$$p(x_{It} \geq \delta_I) = q_{It}\Gamma(x_{It} - \delta_I; 1 + \varepsilon_{It}, c_{It}) + (1 - q_{It})\exp(x_{It} - \delta_I; k_{It}).$$
$$1 \geq q_{It} \geq 0; \varepsilon_{It} = 0; k_{It} > c_{It} > \delta > 0 \quad (4)$$

In Eq. 4, the probability density of a within-bout response is the mixture weight of an exponential distribution (the gamma distribution reduces to an exponential when $\varepsilon_{It} = 0$) with mean c_{It}. The probability of a between-bout response is the mixture weight of an exponential distribution with mean k_{It}. The reciprocal of the means, $1/c_{It}$ and $1/k_{It}$ are the within-bout response rate and bout-initiation rate, respectively. Parameter δ is the minimum IRT in the data for each individual rat and represents the motoric capacity of the subject (Brackney et al., 2011; Killeen, 1994).

The top panel of Fig. 4 shows the mean IRTs for groups FI30 and FI90 as a function of time in the interval; the middle panel shows the same data normalized against the FI duration; the bottom panel shows the mean IRTs for group FI90 as a function of time in the interval during baseline and pre-feeding conditions.

Mean IRTs of both groups decreased as a function of time in the interval. This suggests that the parameters of Eq. 4 do not remain constant over the interval; as the

interval progresses, it is possible that either q_{It} c_{It}, k_{It}, or any combination of these, decay. Eqs. 7-9 account for these changes by assuming that the means of the exponential distributions may decay exponentially starting at time τ, and until some asymptotic IRT, Ω. Furthermore, the mean response-bout length [$1/J_{It} + 1 = 1/(1 - q_{It})$; Cheung et al., 2012] may increase exponentially as a function of the interval. Expressed mathematically,

$$\left.\begin{aligned} J_{It} &= J_{I0} \\ c_{It} &= c_{I0} \\ k_{It} &= k_{I0} \end{aligned}\right\} \quad if\ \tau_I \le t\,,$$

$$\left.\begin{aligned} J_{It} &= J_{I0} e^{-\gamma_i (t-\tau_i)} \\ c_{It} &= (c_{I0} - \Omega_I) e^{-\alpha_I (t-\tau_I)} + \Omega_I \\ k_{It} &= (k_{I0} - \Omega_I) e^{-\beta_I (t-\tau_I)} + \Omega_I \end{aligned}\right\} \quad if\ \tau_I > t\,,$$

$$J_{It}, \gamma_I, \tau_I \ge 0; k_{It} \ge \Omega_I \ge c_{It} \ge 0; \beta_I \ge \alpha_I \ge 0 \quad (5)$$

the meaning of the parameters of Eqs. 4-5 is described in Table 3.

Table 3
IRT Distribution Parameters (Eq. 4-5)

Parameter	Unit	Meaning
$1/J_{It} + 1$	Responses	Mean bout length
c_I	s	Mean within-bout IRT
k_{It}	s	Mean between-bout IRT
Ω_I	s	Asymptotic between-bout IRT
τ_I	s	Time of decay onset
γ_I	s^{-1}	Rate of decay of J_I
α_I	s^{-1}	Rate of decay of c_{It}
β_I	s^{-1}	Rate of decay of k_I
δ_I	s	Minimum IRT

Note. The selected model specified $\alpha_I = 0$.

The results of the model-space investigation are reported in Appendix B and fits to individual rats are reported in Appendix C. Of the nested models tested, Eqs. 4-5 provided the best balance between parsimony and fit to the data when within-bout IRTs, c_{It}, remained constant for both FI30 and FI90. For these conditions, and after correcting for free parameters, this model was at least $e^{1.2}$ times more likely than the most complex model, and at least $e^{3.3}$ times more likely than the next-best simpler model. According to this model, J_{It} and k_{It} decay exponentially beginning at time τ; k_{It} decays to Ω_I. This suggests that the mean bout length increases and the time between bouts decreases to an asymptote as the FI elapses.

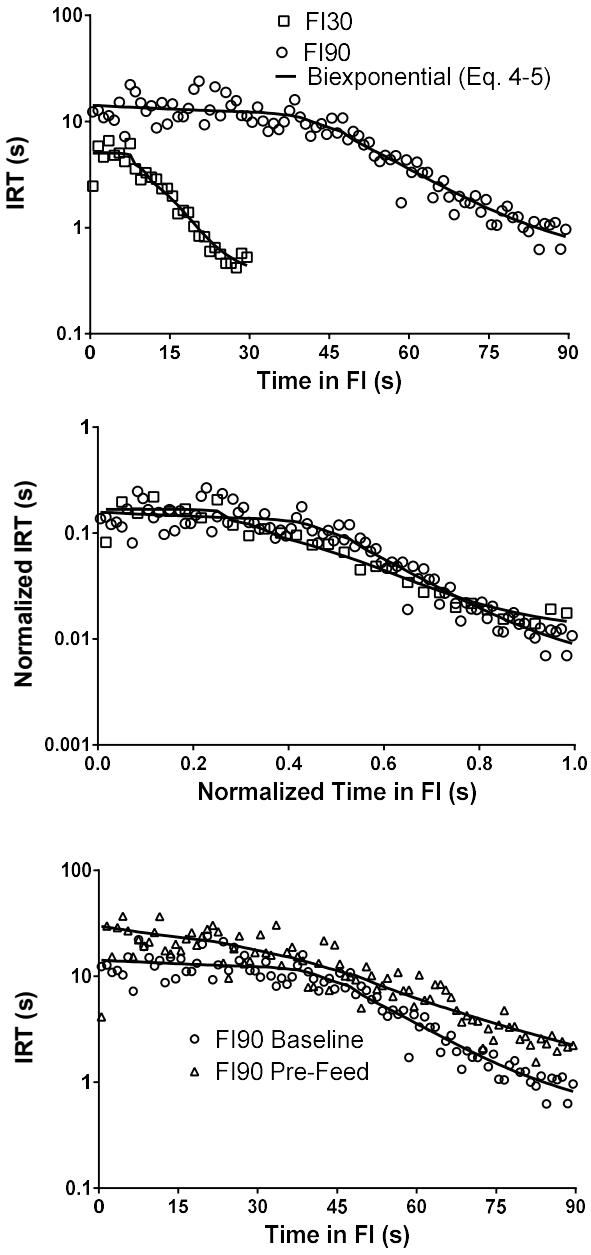

Fig. 4. Top Panel: Mean IRT as a function of time (1-s bins) in the interval for groups FI30 (squares) and FI90 (circles). Middle Panel: Mean normalized IRTs (divided by interval duration) as a function of normalized interval. Normalization was conducted for each rat by representing time as a proportion of the FI. Bottom Panel: Mean IRT as a function of time in the interval for FI90 baseline (circles) and pre-feeding (triangles) performance. Solid lines are mean fitted traces of Eq. 4-5. Note that the y-axis is log base 10 and the x-axis is linear.

Analysis of Schedule and Pre-Feeding Effects on IRTs. Table 4 shows the mean parameter estimates and derived statistics from Eqs. 6-9 for steady-state FI30 and FI90 performance. Grubbs' test revealed the estimate of γ_I and τ_I for rat 1 in FI30 and rat 1 in FI 90, respectively, as outliers, *ps* < .05, and were removed from analysis. Significant differences between groups FI30 and FI90 were detected in estimates of γ_I [t(13) = 5.26, $p < .001$], β_I [t(14) = 2.79, $p = .014$], c_I [t(14) = 2.24, $p = .042$], and τ_I [t(13) = 13.39, $p < .001$]; all other tests were non-significant (*p*s > .050). Specifically, parameters changed more slowly and later, and within-bout IRTs were longer, in FI30 relative to FI90. These results suggest that response-bout length and between-bout IRTs changed more slowly, and the within-bout rate decreased with the longer FI duration.

The distribution parameters of IRTs were assessed at 3 different time-points in the schedule: $t = 0$, t = FI/2 (i.e., 15 and 45 s) and t = FI (i.e., 30 and 90 s) because some parameters, β_I and $1/J_{It} + 1$ decayed and increased, respectively, as the FI elapsed. At t = FI, Grubbs' test revealed the estimate of k_{It} was an outlier for rat 1 in group FI30 ($p < .05$) and was removed from analysis. At every time point estimates of k_{It} and the mean predicted IRT were shorter for FI30 compared to FI 90 [all t(13), t(14) > 2.56, $p < .050$]; all other tests were non-significant (all *p*s > .050). This suggests that only the declining length of between-bout IRTs was consistently shorter in FI 30-s than in FI 90-s performance. The failure to detect a significant difference in bout-length suggests that it is invariant across schedules.

Values in parentheses in Table 4 are parameter estimates divided by their corresponding FI duration. The same outliers as before were detected and removed from the analysis. Rescaled decay parameters (γ_I and β_I) were smaller for FI90 than for FI30

[t(14), t(13) > 3.15, $p < .02$]. Additionally, the rescaled time of decay onset (τ_I) was longer for FI90 than for FI30 [t(13) = 3.96, $p = .001$], rescaled bout-length was shorter for FI90 than FI30 at $t = 0$ and $t = FI/2$ [both t(14) > 5.98, $p < .001$], and the rescaled between-bout IRT and mean predicted IRT was longer for FI90 than FI30 at $t = FI/2$ [both t(14) > 2.27, $p < .038$. No other significant effects of schedule were found for rescaled parameter estimates (all ps > .050). This suggests that the rate at which bout length and between-bout IRTs change in the first half of the interval do not scale with the duration of the FI. These results are consistent with the notion that IRTs, but not their rate of change, are proportional to the FI duration. In particular, estimates of within-bout IRT, between-bout IRT at $t = 0$, and the asymptotic between-bout IRT, appear to scale with the duration of the FI.

In Table 4, the decay of J_I, and k_I are also represented according to their half-lives (e.g. $J_{1/2}$). Once the decay process begins, J_I appears to decay by half after 10-15% of the FI in both FI30 and FI90, whereas k_I appears to decay by half after 10% and 20% of the FI in FI30 and FI90, respectively. The faster decay of J_I suggests that it is the main contributor to the decline in mean IRT observed in Fig. 4. To confirm this intuition, γ_I and β_I were each set to zero while keeping the other parameter at the value reported for each condition in Table 4. Fig. 5 shows the impact of each parameter manipulation on the mean trace of Eqs. 6-9, compared against the mean IRT for FI30 and FI90. Setting $\gamma_I = 0$ and $\beta_I = 0$ increased AICc, respectively, for FI30 by 6055 and 2718, and for FI90 by 50640 and 1231. Parameter half-lives, Fig. 5, and changes in AICc suggest that mean IRTs decline over the course of the FI mainly because response bouts increase in length over the FI.

Table 4

Mean Parameter Estimates and Derived Statistics of the Distribution of IRTs

Parameter	FI 30		FI 90		FI 90 Pre-Feeding	
Decay/Static Param.	*M*	*SEM*	*M*	*SEM*	*M*	*SEM*
c_I	0.261 (0.009)	0.062 (0.002)	0.459 (0.005)	0.094 (0.001)	0.381	0.037
Ω_I	3.024 (0.100)	0.864 (0.029)	6.01 (0.067)	2.221 (0.025)	6.145	2.143
τ_I	8.647 (0.288)	0.675 (0.022)	39.47 (0.439)	2.527 (0.028)	25.079	5.683
γ_I	0.245 (0.008)	0.031 (0.001)	0.075 (0.001)	0.011 (0.001)	0.046	0.009
β_I*	2693667 (89788.89)	1579014 (52633.81)	0.188 (0.002)	0.138 (0.002)	0.051	0.019
$J_{1/2}$	3.341 (0.111)	0.719 (0.024)	10.764 (0.119)	1.565 (0.017)	19.236	3.751
$k_{1/2}$	3.053 (0.101)	1.781 (0.059)	18.696 (0.202)	5.400 (0.059)	31.569	9.822
$t = 0$						
$1/J_{It} + 1$	1.593 (0.053)	0.198 (0.007)	1.649 (0.018)	0.205 (0.002)	1.349	0.043
k_{It}	7.094 (0.236)	1.123 (0.037)	24.743 (0.275)	2.052 (0.023)	32.799	5.476
Mean IRT_t	5.041 (0.168)	1.074 (0.036)	16.794 (0.187)	2.369 (0.026)	20.551	5.029
t = FI / 2						
$1/J_{It} + 1$	2.96 (0.099)	0.606 (0.020)	2.027 (0.023)	0.210 (0.002)	1.975	.122
k_{It}	3.831 (0.128)	0.623 (0.021)	18.366 (0.204)	1.696 (0.019)	19.332	1.745
Mean IRT_t	1.933 (0.064)	0.439 (0.015)	10.069 (0.112)	1.461 (0.016)	9.171	1.509
t = FI						
$1/J_{It} + 1$	101.546 (3.385)	41.353 (1.378)	39.757 (0.442)	15.635 (0.174)	14.189	5.739
k_{It}	3.692 (0.123)	0.706 (0.025)	8.674 (0.096)	1.509 (0.017)	11.855	2.186
Mean IRT_t	0.408 (0.029)	0.109 (0.003)	0.845 (0.009)	0.107 (0.001)	2.221	0.534

Note. See note in Table 3. Parameter $\delta = .005$ for all rats. *Estimates for decay rates can be inordinately high when the decay takes on the form of a step-function, i.e. an abrupt change from baseline to asymptotic parameter values. This was the case for about half of the rats in FI 30 for estimates of β_I.

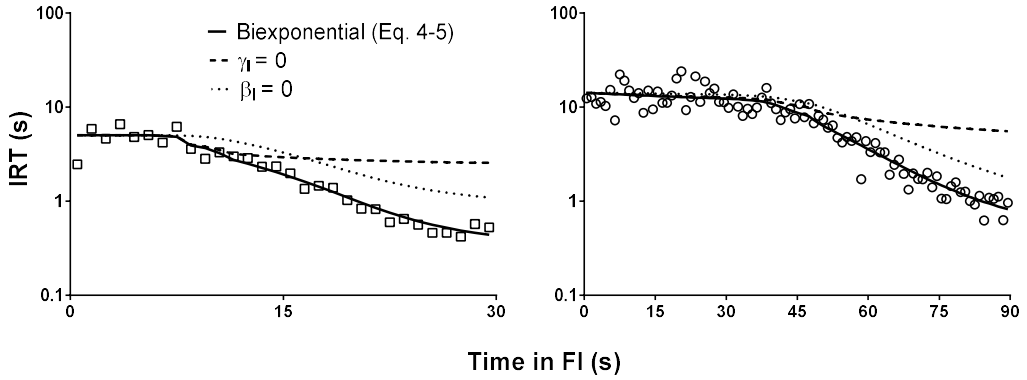

Fig. 5. Mean IRT as a function of time (1-s bins) in the FI for FI30 (left panel) and FI90 (right panel). Lines are mean fitted traces of Eqs. 4-5 (solid), changed so $\gamma_I = 0$ (dashed) and $\beta_I = 0$ (dotted). These curves suggest that the decline of IRTs over the FI is mainly driven by the decay of J_I, i.e., by the increase in bout length. Note that the y-axis is log base 10 and the x-axis is linear.

Table 4 also shows the mean parameter estimates and derived statistics from Eqs. 6-9 for baseline and pre-feeding FI90 performance. Grubbs' test revealed the following estimates as outliers in the FI90 pre-feeding probe: β_I and c_I for rat 6; τ_I for rat 2; $1/J_{It} + 1$ and k_{It} respectively for rats 5 and 2 at $t = 0$, and k_{It} for rat 3 at t = FI/2; all ps < .05. Pre-feeding significantly decreased γ_I [t(7) = 3.51, p = .009] such that bout length increased at a slower rate. At $t = 0$ pre-feeding significantly increased k_{It} [t(6) > 3.35, ps < .02] and the mean IRT [t(7) = 2.64, p < .008]; at t = FI pre-feeding decreased both $1/J_{It} + 1$ [t(7) = 3.51, p = .009] and the mean IRT [t(7) = 3.972, p = .005]; all other tests were non-significant (all ps > .050). These findings suggest that the effects of pre-feeding are largely localized on decreasing the between-bout IRTs (early in the interval) and slowing down the rate of bout lengthening, leaving the rate of within-bout responding relatively intact.

The half-lives of J_I, and k_I may help explain why the effects of pre-feeding on the distribution of IRTs are not observed until later in the interval. It took longer for J_I to decay to half during pre-feeding (20 s) than during baseline (10 s). Furthermore, the half-life of k_I is 10 s longer under pre-feeding (29 s) compared to baseline (19 s). This suggests that pre-feeding slowed down the decline in the prevalence of between-bout IRTs over the interval. Overall, these results suggest that the effect of pre-feeding on parameter estimates observed in the latter portion of the interval are driven by pre-feeding-induced slower lengthening of bouts and an increase in the between-bout IRT.

Response Durations

The top panel of Fig. 8 shows the mean RD of groups FI30 and FI90 as a function of time in the FI; the middle panel shows the mean normalized RD as a function of normalized time; the bottom panel shows the mean RD of group FI90 under baseline and pre-feeding conditions. Interestingly, RDs were generally constant across the duration of the FI (censored by the FI duration). RDs also appear to be roughly proportional to the FI duration and robust to the effects of pre-feeding, although, RDs seem somewhat more variable under pre-feeding conditions.

In the absence of a theory concerning the potential processes governing the duration of a response, RD data was modeled using a dynamic empirical distribution. For each rat in each condition, the FI was divided into 1 s bins. Each bin was populated with RDs that began in that bin. These dynamic empirical distributions allowed for recovery of the response functions shown in Fig. 2 without relying on a mathematical model of RDs.

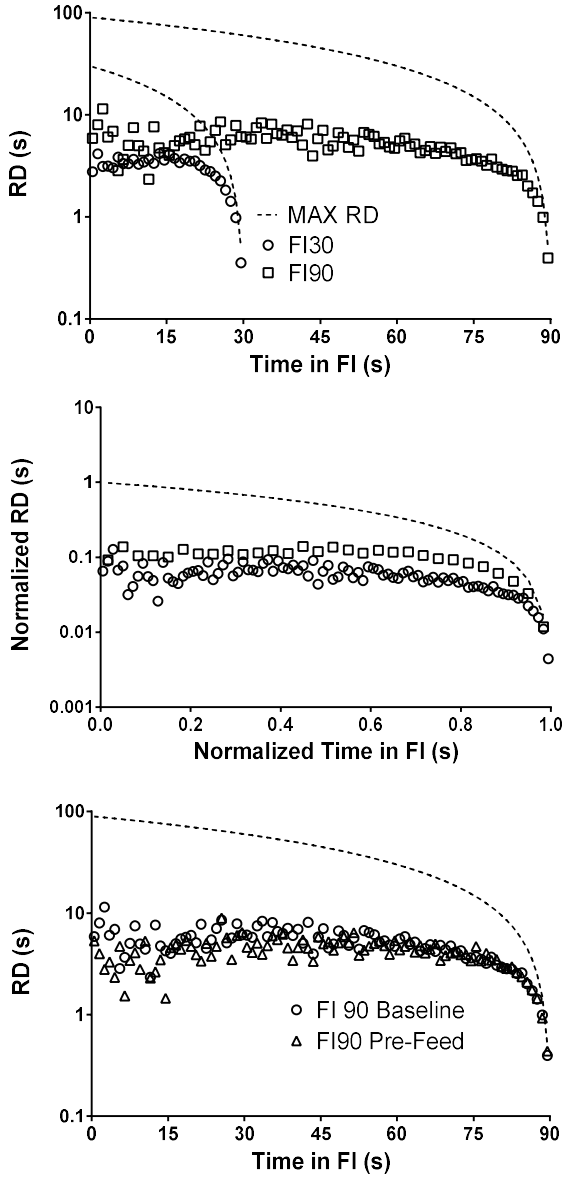

Fig. 6 Top panel: Mean RD as a function of time (1-s bins) in the FI for groups FI30 (squares) and FI90 (circles). Middle Panel: Mean normalized RDs (divided by interval duration) as a function of normalized interval. Normalization was conducted for each rat by representing time as a proportion of the FI. Bottom Panel: Mean RD as a function of time in the interval for FI90 baseline (circles) and pre-feeding (triangles) performance. Note that the y-axis is log base 10 and the x-axis is linear.

Monte Carlo Simulation of Response Functions

The previous sections outlined and evaluated three stochastic models, one for each component of FI performance. To validate that this collection of models accounts for FI performance, a Monte Carlo simulation was conducted using each rat's estimated parameters in each FI and condition in order to reproduce the response functions in Fig. 1.

Fig. 7 shows a schematic of the simulator. In each trial, the simulator first sampled either a timed latency from a gamma distribution ($1+\varepsilon_L$, c_L) with probability q_L, or a non-timed latency from an exponential distribution (k_L) with probability $1 - q_L$. The sampled latency was added to the clock t. Then a RD was sampled from a dynamic empirical distribution (one for each rat in each FI in each condition). The sampled RD was added to t. If $t \geq$ FI (30 s or 90 s), then the trial finished. If $t <$ FI, then either a long IRT was sampled from one exponential distribution (k_{It}) with probability $1 - q_{It}$, or a short IRT was sampled from another exponential distribution (c_{It}) with probability q_{It}. The sampled IRT was added to t; then another RD was sampled, and so on until $t \geq$ FI.

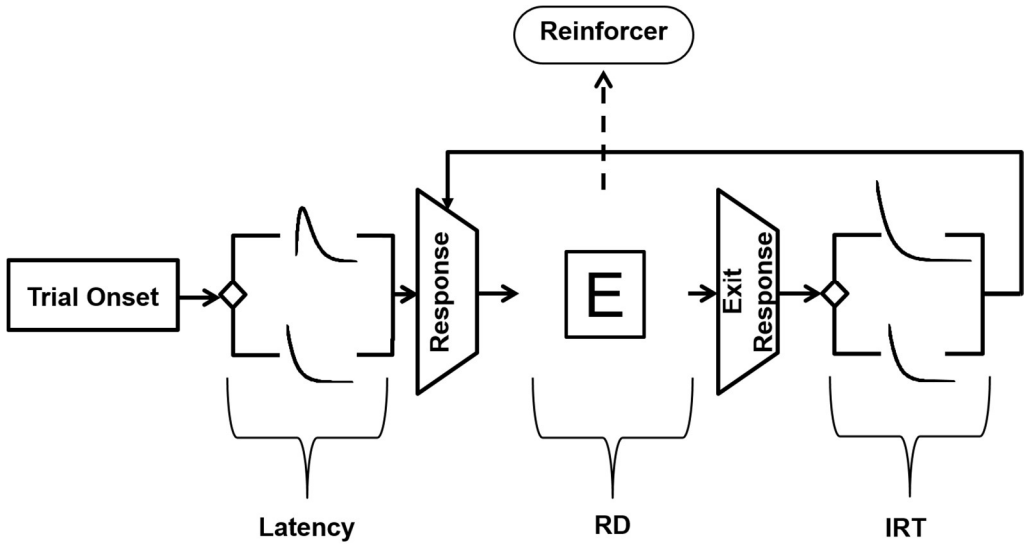

Fig. 7. A generative performance model of FI performance, constructed from the concatenation of latency, RD, and IRT subroutines. Note that the latency and IRT subroutines are Eq. 3 and Eq 4-5, respectively, whereas the RD subroutine samples from the dynamic empirical distribution of RDs, here represented by the letter E.

The simulation was conducted in Matlab (Mathworks, Natick, MA). Each run of the simulator consisted of 295 trials (the approximate number of trials analyzed for each rat); 5000 runs were conducted per rat. Mean response functions ± 2 standard deviations were drawn from these simulations for each rat.

Fig. 8 shows the results of these simulations and Appendix C contains the output of the simulator for each rat. The top row of panels shows the mean observed and simulated response functions in each FI and condition. The second and third rows of panels show the mean observed and simulated response functions of two representative rats from each group and condition. Note that the representative rats in FI90 baseline are the same rats in FI90 pre-feeding. To assess goodness-of-fit both R^2 and norm of residuals were calculated and are reported in Fig. 8 and in the figures of Appendix C. The mean R^2 was .99, .98, and .98; the mean norm of residuals was 0.12, 0.25, and 0.22 for FI30, F90 baseline, and FI90 pre-feeding, respectively. Two rats, rat 1 from FI30 and rat 8 from FI90, were omitted from Fig. 8 based on inspection of R^2 (rat 1: .97; rat 8: .96) and norm of residuals (n.o.r; rat 1: 0.24; rat 8: 0.55) under the baseline condition. In particular, these rats had the smallest R^2 and the largest n.o.r (at least twice as large as the mean). Inspection of the fit of the model to their data confirmed the model in Fig. 7 did not track the empirical response function in those rats as closely as it did in other rats (see Appendix C). Importantly, investigation of the output of the simulator suggests that the model provides an adequate account of the data; almost all observed means are within 2 standard deviations of simulated means.

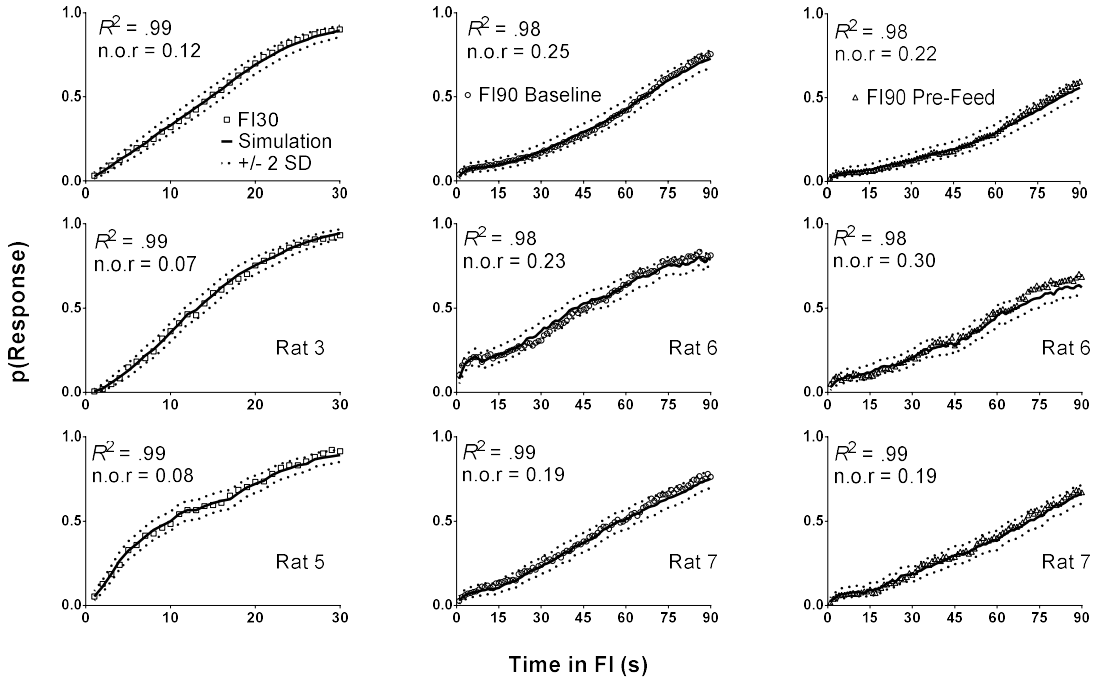

Fig. 8 Top Panels: Mean response functions for each FI and condition as depicted in Fig. 1 plotted against the mean response function (solid line) and ± 2 standard deviations (dashed lines) of the simulator. Each plot also shows R^2 and the norm of residuals (n.o.r). From left to right, the response functions correspond to FI30 (squares), FI90 Baseline (circles), and FI90 pre-feeding (triangles). Middle and Bottom Panels: Response functions for representative rats plotted against the output of the simulator. Note that representative rats for FI90 baseline are also representative rats for FI90 pre-feeding. Response functions were calculated as described in the caption of Fig. 1.

CHAPTER 4

DISCUSSION

The present study separated three components of FI performance: the latency to first response, the inter-response times (IRTs), and the response durations (RDs). Each component was analyzed separately, testing various models nested within a general framework (Eqs. 1 and 2). Taken together, the selected models configure the algorithm depicted in Fig.7, which is a generative performance model of FI performance that adequately reproduces the observed response functions.

Latencies

The analysis of latencies suggests that they are mostly, but not always, *timed* (i.e., gamma distributed, centered on a proportion of the FI). On average, about 80% of latencies were timed with a mean equal to about half the FI. Timed latencies were roughly scalar invariant and robust to changes in reinforcer efficacy. Interestingly, scalar invariance was driven by changes in the scale parameter of the gamma distribution, providing support to the notion that the speed of the clock or at which animal's transition from one state to another decreases as the duration of the FI increases and the rate of reinforcement decreases (Beam, Killeen, Bizo, & Fetterman, 1998; Bizo & White, 1997, 1995, 1994). In contrast, the shape parameter of the gamma distribution (i.e., the response threshold) was not affected by the schedule or a decrease in motivation. Further, the notion that latencies are sensitive to the time between reinforcers is consistent with previous research showing that latencies account for the curvature of FI cumulative records (Gentry et al., 1983), are roughly proportional to the duration of the FI (Shull, 1971; Lowe, Harzem, & Spencer, 1979; Lowe & Wearden, 1981; Wearden, 1985; Zeiler

& Powell, 1994), and track rapid within-session changes in the duration of the FI (Sanabria & Oldenberg, 2014; Ludvig & Staddon, 2004; Higa, 1997; Wynne, Staddon, & Delius, 1996).

The presence of rapid responding at the beginning of a schedule of reinforcement is often referred to as *burst responding* (e.g., Richards, Sabol, & Seiden, 1993) and has been observed in other schedules of reinforcement such as the differential reinforcement of low rates (Richards, et al. 1993; Sanabria & Killeen, 2008), fixed minimum interval (Mazur et al., 2014; Mika et al., 2012; Watterson et al., 2015), dependent concurrent FI FI (Daniels et al., 2015), and lever holding (Sanabria & Killeen, 2008). In these other schedules of reinforcement, burst-generated intervals also appear to be exponentially distributed (e.g., Sanabria & Killeen, 2008). Furthermore, it has been proposed that a random-response component improves the fit of timing models to performance in FI (Lejeune & Warden, 1991), temporal bisection, and temporal generalization procedures (Droit-Volet & Izaute, 2005; Droit-Volet & Wearden, 2001). This suggests that two-state models of timing generally provide a better description than one-state models and thus allow for more accurate inferences.

About 20% of latencies were *not timed* and had a mean of about 1/5th of the FI. These latencies were also scalar invariant but were sensitive to changes in reinforcer efficacy. Specifically, pre-feeding increased both the prevalence and mean of non-timed latencies. Taken together, these findings suggest, contrary to previous research, that parameters governing the distribution of timed responses are robust to changes in motivation, and that the effects of motivation on timing performance reflect changes in its non-timed components.

Inter-Response Times

The analysis of IRTs revealed that their distribution, both in FI 30-s and FI 90-s, was well characterized by a mixture of two exponential distributions with parameters changing exponentially as a function of the passage of time. This characterization is consistent with those of IRTs in non-timing paradigms, such as the variable-interval (VI) schedule of reinforcement (Cheung et al., 2012; Brackney et al. 2011; Shull 2004; Shull et al., 2001, 2002; Fulton, et al., 2001). It suggests that responses are organized in bouts separated by relatively long pauses.

Interestingly, strict adherence to Weber's law was not observed in the parameters governing IRTs. Only two parameters appeared to be scalar invariant: the within-bout IRT and the asymptotic between-bout IRT. This would suggest that peak-rate and asymptotic motivation for the reinforcer scale with the duration of FI. It is unclear why other parameters, and aggregated performance, do not follow Weber's law; nonetheless, systematic departures from Weber's law have been reported (Bizo, Chu, Sanabria & Killeen, 2006; Irvy & Hzeltine, 1995). It is possible that measures of performance consistent with Weber's law are more reflective of scalar-invariant components (peak rate and motivation under high reward expectation) than measures of performance that are inconsistent with Weber's law. Different response topographies (lever pressing vs. head entry) may yield such differences in performance.

Nonetheless, the parameters of the dynamic biexponential model may be intuitively mapped onto features of FI performance. The reciprocal of the within-bout IRT is the rate at which the operant is emitted when rats are seeking food, often expressed as "peak responding" around the time of reinforcement (Roberts, 1981).

Between-bout IRTs may reflect fluctuating levels of motivation which, combined with reinforcement expectancy as expressed in latencies, are low early in the interval (when the subject is engaged in other, interim behaviors), and increase as the time to reinforcement approaches. Bout length appears to grow throughout the interval, suggesting that it may also track reinforcement expectancy. These interpretations are consistent with those drawn from previous research (Brackney et al., 2015, 2011; Cheung et al., 2012).

It seems reasonable to propose, consistent with the two-state description of FI performance proposed by Schneider (1969), the time of decay onset (τ) indicates a stepwise change in expectancy to reinforcement (Gibbon, 1977). However, timed latencies may also index a stepwise change in reinforcer expectancy. Despite the similarity in sensitivity of both parameters to the length of the FI, τ was neither scalar invariant or positively related to timed latencies: estimates of τ were either negatively correlated (in FI 30 s, $r = -.18$) or nearly zero-correlated (in baseline FI 90 s, $0 < r < -.01$) with mean timed latencies. Further research appears to be necessary to establish the distinct psychological significance of τ and timed latencies.

The particularly high sensitivity of response-bout length to the temporal proximity of reinforcement has potential theoretical implications. In particular, response-bout length appears to express a response-reinforcer association that is robust against changes in motivation (Brackney & Sanabria, 2015; Brackney et al., 2011). In support of this interpretation, evidence suggests that food deprivation does not affect VI bout length, and adding a tandem ratio requirement to a VI schedule yields longer response bouts, even though rate of reinforcement is mostly unaffected (Brackney & Sanabria, 2015; Brackney

et al., 2011; Shull et al. 2004, 2001; Shull & Grimes, 2003). The tandem-requirement effect appears to stem from a selective reinforcement of longer bouts (Brackney et al., 2015; Brackney et al., 2011; Killeen, 1969). Changes in bout length during the FI, however, are inconsistent with this explanation. Bouts initiated early in the FI are reinforced only if they are long; such selective reinforcement should yield shorter bouts as the FI elapses, which is the opposite of what was observed. Moreover, bouts proximal to reinforcement appear to be sensitive to changes in reinforcer efficacy in the FI 90-s schedule.

A potential solution to these inconsistencies posits that the response-reinforcer association reflected in the length of bouts is directly related to the underlying associative structure supported by the schedule and is modulated by reinforcer efficacy. In VI schedules, the distribution of intervals between trial onset and reinforcement is typically exponential. This distribution yields a constant subjective hazard function of reinforcement—i.e., a constant subjective expectation that reinforcement is available *now*. In contrast, the subjective hazard function of reinforcement supported by FI schedules is likely positive, increasing as the FI increases (Machado, 1997; Kirkpatrick, 2002; Staddon, Chelaru, & Higga, 2002; Dragoi, Staddon, Palmer, & Buhusi, 2003). It is possible that bout length is shaped by reinforcement (thus explaining tandem-requirement effects in VI schedules), but also reflects the subjective hazard function of reinforcement (thus explaining the within-trial pattern of growth in FI schedules).

There are two likely explanations for the pre-feeding-induced shortening of bout lengths estimated at the time of reinforcement. The first explanation is that this is a mathematical artifact. Reinforcement terminates the ongoing response bout, so its

uncensored length is estimated from the pattern of change of response bouts over the FI. It is possible that this estimation is flawed in such way as to predict shorter (censored) bouts when bouts are infrequent, such as under pre-feeding. The second explanation is that the interaction of reinforcer expectation and motivation directly affect bout length. It is possible that when the expectation of reinforcement is low (as in VI schedules and early in FI trials), changes in motivation do not affect bout length, but when the expectation is high, they do. Future research may test this latter hypothesis.

Response Durations

Unlike latencies and IRTs, RDs were not modeled and the empirical distribution was used to recover aggregate behavior. We sought to provide a reasonable description of RDs that, along with latency and IRT parameters, would allow us to program a simulator of FI performance (Fig. 7). Nonetheless, the data reported here merits a few qualitative observations. First, the duration of FI-reinforced head entries appears to be relatively constant across the FI, This observation is in contrast to previous reports suggesting the duration of a lever press decreases as the time to reinforcement approaches (Roberts & Gharib, 2006). Second, RDs do not appear to be sensitive to changes in reinforcer efficacy. These observations are potentially informative and useful for the development of theoretical models of operant response duration (e.g., Hurwitz, 1954; Gharib, Derby, & Roberts, 2000).

Implications for Timing Research

The concatenation of the stochastic processes underlying latencies and IRTs resulted in a comprehensive generative FI performance model. This model adequately reproduced response functions of individual animals as well as mean response functions.

The success of the simulator suggests that the proposed generative model provides a viable route by which to understand FI behavior. Further, it is consistent with previous attempts to characterize schedule-controlled behavior in terms of two-state Markov models (Harris, 2015; Brackney et al., 2011; Shull et al., 2001; Gibbon, 1995; Meyerson & Miezein, 1980).

For example, Harris (2015) compared two models of aggregate FT performance, a two-state and a continuous change model; within both models was a nested mixture model in which according to some probability animals would be in an engaged state (emitting a response) and with a complimentary probability a disengaged state (not emitting a response). In the two-state model, the probability of entering an engaged state increased and in the continuous-change model, the probability of entering an engaged state remained constant but the rate of responding in the engaged state increased as the interval elapsed. He found that the two-state model provided the best description of aggregated data and is conceptually similar to the present finding that what drives the decay of IRTs is a progressive lengthening of bout length (i.e. a progressive increase in the probability of a within-bout IRT). However, our microstructural analysis revealed both bout length and between-bout IRTs needed to increase and decrease, respectively, as the interval elapsed to account for the microstructure of the data. This suggests a complexity to the data otherwise missed if analyses are restricted to aggregate performance (Hanson & Killeen, 1981).

The proposed generative model of FI performance also suggests that temporal control in FI schedules is confined to a subset of latencies and, therefore, estimates of such control may be isolated from potentially confounding processes. Such dissociation

provides an alternative characterization of performance in a common timing paradigm, the peak-interval procedure. Previous research suggests that the mean and dispersion of peak-interval gradients isolate key features of the control that periodic reinforcement exerts over behavior (Roberts, 1981; Buhusi & Meck, 2005). That is, all responses observed in the peak procedure are generated by a timing mechanism. However, recent research suggests that these features may be best characterized by the distribution of latencies, or start-times (Taylor, Horvitz, & Balsam, 2007; Saulsgiver, McClure, & Wynne, 2006; but see Balci, Ludvig, & Brunner, 2010 for a discussion of stop-times as a potential measure). This revised interpretation of peak performance, i.e. that temporal performance may be best characterized by the distribution of start-times rather than aggregate response functions, is consistent with present findings that suggest that (a) the response run is characterized by random bouts of responding instead of a timing process, and (b) only a subset of latencies is sensitive to the periodicity of reinforcement. These findings suggest that the peak procedure conflates motivation and timing (Sanabria et al., 2009; Daniels et al., 2015a).

The dissociation of processes underlying latencies and response runs also sheds light on previous research that suggests that peak-interval performance is sensitive to changes in reinforcer efficacy. Such sensitivity is demonstrated by horizontal shifts in the peak-interval gradient and the distribution of latencies (e.g. Galtress, Marshall, & Kirkpatrick, 2012; Galtress & Kirkpatrick, 2009; Belke & Christie-Fougere, 2006; Ludvig, Conover, & Shizgal, 2007; Plowright, Church, Behnke, & Silverman, 2000). Based on these effects, it has been theorized that motivation and timing processes are intimately connected, and thus interact to produce overt behavior (Kirkpatrick, 2014).

The present study suggests an alternative explanation: the horizontal shift in the distribution of latencies and in the peak-interval gradient are likely due to a decrease in the prevalence of timed-latencies, an increase in the mean of non-timed latencies, and a shortening of response bouts around the time when reinforcement is anticipated. These changes do not imply a change in timing; instead, they suggest a reduction in motivation for the reinforcer, which results in reduced temporal control and response rate. Furthermore, this suggestion is consistent with the notion that reduction in motivation for the reinforcer alters preference for engaging in the FI over alternative behaviors (Killeen & Pellon, 2013, Sanabria et al., 2009; Gibbon, 1995)

The present generative performance model is consistent, to some extent, with the Packet theory of timing (Guilhardi, Yi, & Church, 2007; Church & Guilhardi, 2005; Guilhardi & Church, 2005; Guilhardi, Keen, MacInnis, & Church, 2005; Kirkpatrick & Church, 2003; Kirkpatrick, 2002; also see Dragoi, et al., 2013 for an alternative to Packet Theory). Packet theory is the only theory of timing to operate on the assumption of bout-like behavior; it stipulates that responding in interval schedules of reinforcement is a composite of the temporal structure of bouts and the rate at which bouts are generated. According to Packet theory, what drives the increasing response rate across the FI is the increased expectation for the reinforcer, which yields an increased probability of a bout. Implementations of the theory produce response bouts such that, if in the middle of a bout another bout is generated, then that new bout is concatenated with the previous bout (Kirkpatrick, 2002); the concatenation of bouts therefore increases as the FI elapses. This process is reflected in the proposed IRT model as an increase in bout length over the

course of the FI, and is consistent with our suggestion that bout length reflects the subjective hazard function of reinforcement supported by the schedule.

There are, however, a few important differences between the present model and Packet Theory. Packet Theory assumes that (a) latencies are not differentiated from IRTs, (b) latencies and IRTs are both described by a Wald distribution suggesting both arise from a timing process, and (c) only the probability of a bout changes as a function of time in the FI. Assumptions a and b are in conflict with the present data and previous research suggesting that behavior fluctuates into and out of states of schedule control, and that latencies and run rate characterize two different processes. To address the present data, Packet Theory would infer that pre-feeding affects the timing process. Assumption c is inconsistent with the decrease in between-bout IRTs over the FI, suggested by the present data, but may actually emerge out of the dynamics of Packet Theory.

Limitations and Future Directions

A potential limitation of the proposed model is it is agnostic regarding correlations within and between components of FI performance (e.g., consecutive latencies, consecutive IRTs and RDs), and was evaluated without taking those potential sequential dependencies into consideration. Prior research has shown interesting patterns of sequential dependency between latencies (Shull, 1971) and between IRTs (Gentry, et al., 1983). Furthermore, recent research has revealed that even after animals are well trained, both latencies and run rates may change as a function of time in the session (Balci, et al., 2010). Future developments of the proposed generative model may incorporate the relation between components of FI performance, and their changes within each session.

Conclusion

The present study provides evidence that timing processes may be isolated from other confounding processes using established models of operant performance. Timing processes appear to be expressed in a subset of latencies to the first response, whose distribution is scale-invariant and robust against changes in reinforcer efficacy. Response runs appear to be organized in bouts whose length increases as the time to reinforcement approaches. The dissociation of these components of FI performance, and the observation that pre-feeding does not directly affect timed latencies, provides useful insights into the relation between timing and motivation, and for the development of analytical tools for testing hypotheses regarding timing and its sensitivity to reward value (Galtress & Kirkpatrick, 2009; Ludvig, Conover & Shizgal, 2007; Plowright, Church, Behnke & Silverman, 2000). Specifically, timing and motivation appear to be dissociable components of interval timing. Although these tools were applied to a limited range of data in the present study, the analytical models are beneficial in that they derive from a single general equation and have already been tested in other schedules of reinforcement. Moreover, the present generative performance model suggests that models of timing are still incomplete. It highlights the need to refine our understanding of the microstructure of FI performance.

REFERENCES

Avlar, B., Kahn, J. B., Jensen, G., Kandel, E. R., Simpson, E. H., & Balsam, P. D. (2015). Improving temporal cognition by enhancing motivation. Behavioral Neuroscience, 129(5), 576.

Balcı, F. (2014). Interval Timing, Dopamine, and Motivation. Timing & Time Perception, 2(3), 379-410.

Balci, F., Ludvig, E. A., Abner, R., Zhuang, X., Poon, P., & Brunner, D. (2010). Motivational effects on interval timing in dopamine transporter (DAT) knockdown mice. Brain research, 1325, 89-99.

Balci, F., Ludvig, E. A., & Brunner, D. (2010). Within-session modulation of timed anticipatory responding: When to start responding. Behavioural processes, 85(2), 204-206.

Beam, J. J., Killeen, P. R., Bizo, L. A., & Fetterman, J. G. (1998). How reinforcement context affects temporal production and categorization. Animal Learning & Behavior, 26, 388-396.

Belke, T. W., & Christie-Fougere, M. M. (2006). Investigations of timing during the schedule and reinforcement intervals with wheel-running reinforcement.Behavioural processes, 73(3), 240-247.

Berridge, K. C., & Kringelbach, M. L. (2013). Neuroscience of affect: brain mechanisms of pleasure and displeasure. Current opinion in neurobiology, 23(3), 294-303.

Bizo, L. A., Chu, J. Y., Sanabria, F., & Killeen, P. R. (2006). The failure of Weber's law in time perception and production. Behavioural Processes, 71(2), 201-210.

Bizo, L. A., & White, K. G. (1997). Training with controlled reinforcer density: Implications for models of timing. Journal of Experimental Psychology: Animal Behavior Processes, 23, 44.

Bizo, L. A., & White, K. G. (1995). Reinforcement context and pacemaker rate in the behavioral theory of timing. Animal Learning & Behavior, 23, 376-382.

Bizo, L. A., & White, K. G. (1994). The behavioral theory of timing: Reinforcer rate determines pacemaker rate. Journal of the Experimental Analysis of Behavior, 61, 19-33.

Brackney, R. J., & Sanabria, F. (2015). The distribution of response bout lengths and its sensitivity to differential reinforcement. Journal of the Experimental Analysis of Behavior, 104(2), 167-185.

Brackney, R. J., Cheung, T. H., Neisewander, J. L., & Sanabria, F. (2011). The isolation of motivational, motoric, and schedule effects on operant performance: a modeling approach. Journal of the experimental analysis of behavior, 96(1), 17-38.

Buhusi, C. V., & Meck, W. H. (2005). What makes us tick? Functional and neural mechanisms of interval timing. Nature Reviews Neuroscience, 6(10), 755-765.

Burnham, K. P., & Anderson, D. R. (2002). Model selection and multimodel inference: a practical information-theoretic approach. Springer Science & Business Media.

Cabrera, F., Sanabria, F., Jiménez, Á. A., & Covarrubias, P. (2013). An affordance analysis of unconditioned lever pressing in rats and hamsters. Behavioural processes, 92, 36-46.

Catania, A. C. (1970). Reinforcement schedules and psychophysical judgments: A study of some temporal properties of behavior. The theory of reinforcement schedules, 1-42.

Church, R. M., & Guilhardi, P. (2005). A Turing test of a timing theory. Behavioural processes, 69(1), 45-58.

Cheung, T. H., Neisewander, J. L., & Sanabria, F. (2012). Extinction under a behavioral microscope: isolating the sources of decline in operant response rate. Behavioural processes, 90(1), 111-123.

Conover, K. L., Fulton, S., & Shizgal, P. (2001). Operant tempo varies with reinforcement rate: implications for measurement of reward efficacy. Behavioural processes, 56(2), 85-101.

Coull, J. T., Hwang, H. J., Leyton, M., & Dagher, A. (2012). Dopamine precursor depletion impairs timing in healthy volunteers by attenuating activity in putamen and supplementary motor area. The Journal of Neuroscience, 32(47), 16704-16715.

Daniels, C. W., Watterson, E., Garcia, R., Mazur, G. J., Brackney, R. J., & Sanabria, F. (2015a). Revisiting the effect of nicotine on interval timing. Behavioural brain research, 283, 238-250.

Daniels, C. W., Fox, A. E., Kyonka, E. G., & Sanabria, F. (2015b). Biasing Temporal Judgments in Rats, Pigeons, and Humans. International Journal of Comparative Psychology.

Dragoi, V., Staddon, J. E. R., Palmer, R. G., & Buhusi, C. V. (2003). Interval timing as an emergent learning property. Psychological Review, 110(1), 126.

Droit-Volet, S., & Izaute, M. (2005). The effect of feedback on timing in children and adults: The temporal generalization task. The Quarterly Journal of Experimental Psychology Section A, 58(3), 507-520.

Droit-Volet, S., & Wearden, J. H. (2001). Temporal bisection in children. Journal of Experimental Child Psychology, 80(2), 142-159.

Freestone, D. M., Balcı, F., Simen, P., & Church, R. M. (2015). Optimal response rates in humans and rats. Journal of Experimental Psychology: Animal Learning and Cognition, 41(1), 39.

Gibbon, J. (1995). Dynamics of time matching: Arousal makes better seem worse. Psychonomic Bulletin & Review, 2(2), 208-215.

Galtress, T., Marshall, A. T., & Kirkpatrick, K. (2012). Motivation and timing: clues for modeling the reward system. Behavioural processes, 90(1), 142-153.

Galtress, T., & Kirkpatrick, K. (2010). The role of the nucleus accumbens core in impulsive choice, timing, and reward processing. Behavioral neuroscience,124(1), 26.

Gentry, G. David, Bernard Weiss, and Victor G. Laties. The microanalysis of fixed-interval responding. Journal of the Experimental Analysis of Behavior 39.2 (1983): 327-343.

Gharib, A., Derby, S., & Roberts, S. (2001). Timing and the control of variation. Journal of Experimental Psychology: Animal Behavior Processes, 27(2), 165.

Guilhardi, P., Yi, L., & Church, R. M. (2007). A modular theory of learning and performance. Psychonomic Bulletin & Review, 14(4), 543-559.

Guilhardi, P., & Church, R. M. (2005). Dynamics of temporal discrimination. Learning & behavior, 33(4), 399-416.

Guilhardi, P., Keen, R., MacInnis, M. L., & Church, R. M. (2005). How rats combine temporal cues. Behavioural processes, 69(2), 189-205.

Hanson, S. J., & Killeen, P. R. (1981). Measurement and modeling of behavior under fixed-interval schedules of reinforcement. Journal of Experimental Psychology: Animal Behavior Processes, 7(2), 129.

Harris, J. A. (2015). Changes in the Distribution of Response Rates Across the CS-US Interval: Evidence that Responding Switches Between Two Distinct States.

Higa, J. J. (1997). Rapid timing of a single transition in interfood interval duration by rats. Animal Learning & Behavior, 25(2), 177-184.

Hill, J. C., Herbst, K., & Sanabria, F. (2012). Characterizing operant hyperactivity in the Spontaneously Hypertensive Rat. Behavioral and Brain Function, 8(5), 1-15.

Hurwitz, H. M. B. (1954). Response-duration of lever pressing in the rat. Quarterly Journal of Experimental Psychology, 6(2), 62-71.

Íbias, J., Pellón, R., & Sanabria, F. (2015). A microstructural analysis of schedule-induced polydipsia reveals incentive-induced hyperactivity in an animal model of ADHD. Behavioural Brain Research, 278, 417-423.

Ivry, R. B., & Hazeltine, R. E. (1995). Perception and production of temporal intervals across a range of durations: evidence for a common timing mechanism. Journal of Experimental Psychology: Human Perception and Performance, 21(1), 3.

Kalafut, K. L., Freestone, D. M., MacInnis, M. L., & Church, R. M. (2014). Integrating timing and conditioning approaches to study behavior. Journal of Experimental Psychology: Animal Learning and Cognition, 40(4), 431.

Karmarkar, U. R., & Buonomano, D. V. (2007). Timing in the absence of clocks: encoding time in neural network states. Neuron, 53(3), 427-438.

Killeen, P. R., & Sitomer, M. T. (2003). MPR. Behavioural Processes, 62(1), 49-64.

Killeen, P. R., Hall, S. S., Reilly, M. P., & Kettle, L. C. (2002). Molecular analyses of the principal components of response strength. Journal of the Experimental Analysis of Behavior, 78(2), 127-160.

Killeen, P. R. (1994). Mathematical principles of reinforcement. Behavioral and Brain Sciences, 17(01), 105-135.

Killeen, P. R., & Fetterman, J. G. (1988). A behavioral theory of timing. Psychological review, 95(2), 274.

Killeen, P. (1969). Reinforcement frequency and contingency as factors in fixed-ratio behavior. Journal of the Experimental analysis of Behavior, 12(3), 391-395.

Kirkpatrick, K. (2014). Interactions of timing and prediction error learning. Behavioural processes, 101, 135-145.

Kirkpatrick, K., & Church, R. M. (2003). Tracking of the expected time to reinforcement in temporal conditioning procedures. Learning & Behavior, 31(1), 3-21.

Kirkpatrick, K. (2002). Packet theory of conditioning and timing. Behavioural Processes, 57(2), 89-106.

Lejeune, H., & Wearden, J. H. (1991). The comparative psychology of fixed-interval responding: some quantitative analyses. Learning and Motivation,22(1), 84-111.

Lowe, C. F., & Wearden, J. H. (1981). Weber law and the fixed-interval post-reinforcement pause. Behaviour Analysis Letters,1(1), 27-32.

Lowe, C. F., Harzem, P., & Spencer, P. T. (1979). Temporal control of behavior and the power law. Journal of the Experimental Analysis of Behavior, 31(3), 333-343.

Ludvig, E. A., Balci, F., & Spetch, M. L. (2011). Reward magnitude and timing in pigeons. Behavioural processes, 86(3), 359-363.

Ludvig, E. A., Conover, K., & Shizgal, P. (2007). The effects of reinforcer magnitude on timing in rats. Journal of the experimental analysis of behavior,87(2), 201-218.

Ludvig, E. A., & Staddon, J. E. (2004). The conditions for temporal tracking under interval schedules of reinforcement. Journal of Experimental Psychology: Animal Behavior Processes, 30(4), 299.

Machado, A., Malheiro, M. T., & Erlhagen, W. (2009). Learning to time: A perspective. Journal of the Experimental Analysis of Behavior, 92(3), 423-458.

Machado, A. (1997). Learning the temporal dynamics of behavior. Psychological review, 104(2), 241.

Mazur, G. J., Wood-Isenberg, G., Watterson, E., & Sanabria, F. (2014). Detrimental effects of acute nicotine on the response-withholding performance of spontaneously hypertensive and Wistar Kyoto rats. Psychopharmacology,231(12), 2471-2482.

Myerson, J., & Miezin, F. M. (1980). The kinetics of choice: An operant systems analysis. Psychological Review, 87(2), 160.

Mika, A., Mazur, G. J., Hoffman, A. N., Talboom, J. S., Bimonte-Nelson, H. A., Sanabria, F., & Conrad, C. D. (2012). Chronic stress impairs prefrontal cortex-dependent response inhibition and spatial working memory. Behavioral neuroscience, 126(5), 605.

Molet, M., & Miller, R. R. (2014). Timing: an attribute of associative learning. Behavioural processes, 101, 4-14.

Myung, I. J. (2003). Tutorial on maximum likelihood estimation. Journal of mathematical Psychology, 47(1), 90-100.

Oprisan, S. A., & Buhusi, C. V. (2011). Modeling pharmacological clock and memory patterns of interval timing in a striatal beat-frequency model with realistic, noisy neurons. Frontiers in integrative neuroscience, 5.

Pavlov, I.P. (1927). Conditioned Reflexes (G.V. Anrep, Trans.). London, UK: Oxford University Press.

Plowright, C. M. S., Church, D., Behnke, P., & Silverman, A. (2000). Time estimation by pigeons on a fixed interval: the effect of pre-feeding. Behavioural processes, 52(1), 43-48.

Rescorla, R. A. (1967). Inhibition of delay in Pavlovian fear conditioning.Journal of comparative and physiological psychology, 64(1), 114.

Richards, J. B., Sabol, K. E., & Seiden, L. S. (1993). DRL interresponse-time distributions: Quantification by peak deviation analysis. Journal of the experimental analysis of behavior, 60(2), 361-385.

Roberts, S. (1981). Isolation of an internal clock. Journal of Experimental Psychology: Animal Behavior Processes, 7(3), 242.

Sanabria, F., & Oldenburg, L. (2014). Adaptation of timing behavior to a regular change in criterion. Behavioural processes, 101, 58-71.

Sanabria, F., Thrailkill, E. A., & Killeen, P. R. (2009). Timing with opportunity cost: Concurrent schedules of reinforcement improve peak timing. Learning & behavior, 37(3), 217-229.

Sanabria, F., & Killeen, P. R. (2008). Evidence for impulsivity in the Spontaneously Hypertensive Rat drawn from complementary response-withholding tasks. Behav Brain Funct, 4(7).

Saulsgiver, K. A., McClure, E. A., & Wynne, C. D. L. (2006). Effects of d-amphetamine on the behavior of pigeons exposed to the peak procedure.Behavioural processes, 71(2), 268-285.

Shull, R. L. (2004). Bouts of responding on variable-interval schedules: effects of deprivation level. Journal of the Experimental Analysis of Behavior, 81(2), 155-167.

Shull, R. L., Grimes, J. A., & Bennett, J. A. (2004). Bouts of responding: the relation between bout rate and the rate of variable-interval reinforcement. Journal of the experimental analysis of behavior, 81(1), 65-83.

Shull, R. L., Gaynor, S. T., & Grimes, J. A. (2001). Response rate viewed as engagement bouts: Effects of relative reinforcement and schedule type. Journal of the experimental analysis of behavior, 75(3), 247-274.

Shull, R. L., Gaynor, S. T., & Grimes, J. A. (2002). Response rate viewed as engagement bouts: Resistance to extinction. Journal of the experimental analysis of behavior, 77(3), 211-231.

Shull, R. L. (1971). Sequential patterns in post-reinforcement pauses on fixed-interval schedules of food. Journal of the Experimental Analysis of Behavior, 15(2), 221-231.

Simen, P., Rivest, F., Ludvig, E. A., Balci, F., & Killeen, P. (2013). Timescale invariance in the pacemaker-accumulator family of timing models. Timing & Time Perception, 1(2), 159-188.

Simen, P., Balci, F., Cohen, J. D., & Holmes, P. (2011). A model of interval timing by neural integration. The Journal of Neuroscience, 31(25), 9238-9253.

Skinner, B.F. (1938). The behavior of organisms. Cambridge, MA: Copley Publishing Group.

Smith, T. T., McLean, A. P., Shull, R. L., Hughes, C. E., & Pitts, R. C. (2014). Concurrent performance as bouts of behavior. Journal of the experimental analysis of behavior, 102(1), 102-125.

Staddon, J. E. R. (2005). Interval timing: memory, not a clock. Trends in cognitive sciences, 9(7), 312-314.

Staddon, J. E. R., Chelaru, I. M., & Higa, J. J. (2002). Habituation, memory and the brain: The dynamics of interval timing. Behavioural Processes, 57(2), 71-88.

Staddon, J. E. R., & Higa, J. J. (1999). Time and memory: towards a pacemaker-free theory of interval timing. Journal of the experimental analysis of behavior, 71(2), 215-251.

Taylor, K. M., Horvitz, J. C., & Balsam, P. D. (2007). Amphetamine affects the start of responding in the peak interval timing task. Behavioural processes,74(2), 168-175.

Treisman, M. (1963). Temporal discrimination and the indifference interval: Implications for a model of the" internal clock". Psychological Monographs: General and Applied, 77(13), 1.

Vogel, E. H., Brandon, S. E., & Wagner, A. R. (2003). Stimulus representation in SOP:: II. An application to inhibition of delay. Behavioural Processes, 62(1), 27-48.

Watterson E., Mazur G.J., & Sanabria F. (in press). Validation of a method to assess ADHD-related impulsivity in animal models. Journal of Neuroscience Methods.

Wearden, J. H. (1985). The power law and Weber's law in fixed-interval postreinforcement pausing: A scalar timing model. The Quarterly Journal of Experimental Psychology, 37(3), 191-211.

Wynne, C. D., Staddon, J. E., & Delius, J. D. (1996). Dynamics of waiting in pigeons. Journal of the experimental analysis of behavior, 65(3), 603-618.

Zeiler, M. D., & Powell, D. G. (1994). Temporal control in fixed-interval schedules. Journal of the Experimental Analysis of Behavior,61(1), 1-9.

APPENDIX A

MODEL SELECTION

A model-space investigation was conducted using data from each group of rats under baseline conditions to determine which free parameters in Eq. 1 and 2 were justified for each component of FI performance. All potential nested models of each component of FI performance (Eq. 1 (also see Eq. 3) for latencies, Eq. 1 and 2 (also see Eq. 4-5) for IRTs) were fit to the data of each rat from group FI30 and FI90 using the method of maximum likelihood (Myung, 2003). For each model, the maximum log-likelihood estimate (MLE) was used to compute the corrected Akaike Information Criterion (AICc; Burnham & Anderson, 2002). Briefly, AICc favors nested models that balance goodness-of-fit (higher MLE) against parsimony (fewer free parameters); lower AICc are indicative of better balance. The analysis yielded a selection criterion ΔAICc for each nested model; ΔAICc of nested model *i* is the AICc of nested model *i* minus the lowest AICc across all models compared. Thus, the nested model with the lowest AICc has a ΔAICc = 0 and all other nested models have a ΔAICc > 0. The simplest constrained nested models within 4 ΔAICc units of the minimum ΔAICc were selected (this threshold is recommended by other researchers; see Bunrhman & Anderson, 2002; Brackney et al., 2011) as the most likely model providing the best balance of fit (low AICc) and parsimony (fewest free parameters).

APPENDIX B

MODEL SELECTION OUTCOMES

Table B1

Latency Model Selection

Group	Model	# of Free Parameters	MLE	AICc	ΔAICc
FI 30	q_L, ε_L, c_L, k_L	32	-7558.69	15182.31	0*
	$q_L = 1$, ε_L, c_L	16	-7648.77	15401.76	219.49
	$q_L = 0$, k_L	8	-8065.11	16146.29	1284.04
FI 90	q_L, ε_L, c_L, k_L	32	-10333.50	20731.92	0*
	$q_L = 1$, ε_L, c_L	16	-10675.54	21399.60	667.69
	$q_L = 0$, k_L	8	-10908.78	21833.62	1101.70

Note. Models are labeled with the parameters that were allowed to vary. The number of free parameters for each model is equal to the number of free parameters allowed to vary times the number of rats (8). Models were fit to 2360 data points for FI 30 and for FI 90 (~295 per rat). *The model with the fewest free parameters and a ΔAICc < 4 was selected for each group.

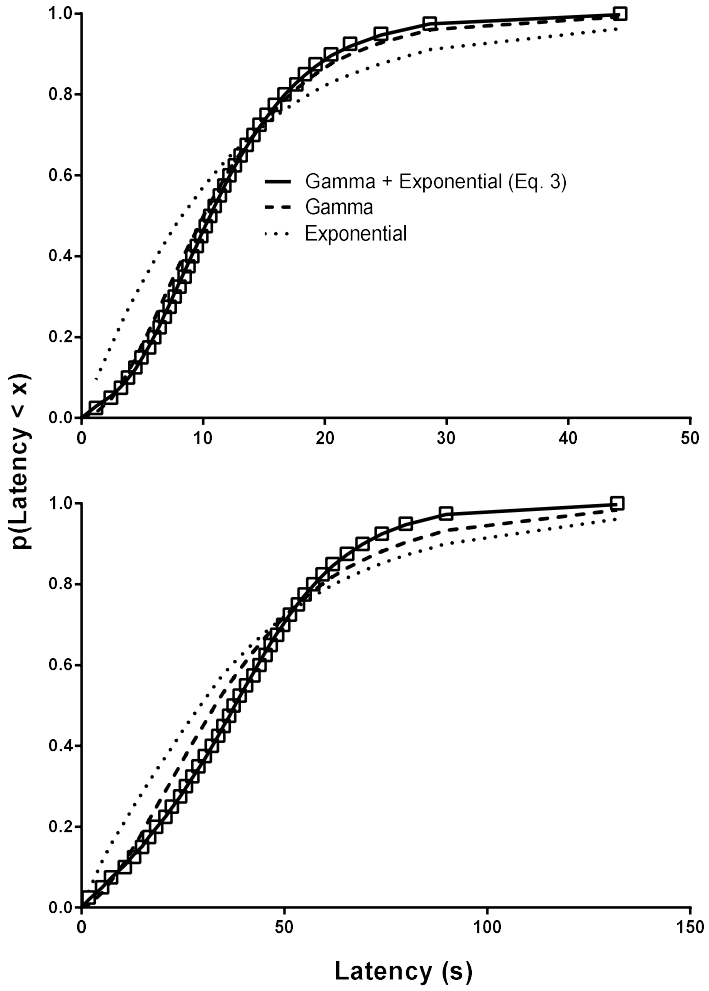

Fig. B1. Left panel: Mean empirical cumulative distribution of latencies (squares) from each FI and mean fit of each model in Table B1: gamma + exponential (solid line), gamma (dashed line), exponential (dotted line). Latencies are organized in 40 bins of equal number of latencies.

Table B2
IRT Model Selection

Group	Model	# of Free Parameters	MLE	AICc	ΔAICc
FI 30	J_{I0}, $c_{I0} = k_{I0}$	8	-9338.13	19892.27	14745.50
	J_{I0}, $c_{I0} = k_{I0}$, $\alpha_I = \beta_I$	24	-4299.37	8646.73	3500.06
	J_{I0}, c_{I0}, k_{I0},	24	-3953.15	7954.29	2807.62
	J_{I0}, c_{I0}, k_{I0}, γ_I	32	-3145.43	6354.86	1208.26
	J_{I0}, c_{I0}, k_{I0}, $\alpha_I = \beta_I$	32	-3439.26	6942.52	1795.92
	J_{I0}, c_{I0}, k_{I0}, α_I	32	-3684.10	7432.21	2285.61
	J_{I0}, c_{I0}, k_{I0}, γ_I, $\alpha_I = \beta_I$	40	-2957.56	5995.12	848.63
	J_{I0}, c_{I0}, k_{I0}, γ_I, α_I	40	-3130.44	6340.88	1194.39
	J_{I0}, c_{I0}, k_{I0}, α_I, β_I	40	-3429.25	6938.50	1792.01
	J_{I0}, c_{I0}, k_{I0}, γ_I, α_I, β_I	48	-2956.72	6009.43	863.07
	J_{I0}, c_{I0}, k_{I0}, γ_I, α_I, β_I, Ω_I	56	-2846.15	5804.31	658.09
	J_{I0}, c_{I0}, k_{I0}, γ_I, α_I, β_I, Ω_I, δ_I	56	-2535.92	5183.85	37.63
	J_{I0}, c_{I0}, k_{I0}, γ_I, α_I, β_I, Ω_I, δ_I, τ_I	64	-2509.03	5146.05	0
	J_{I0}, c_{I0}, k_{I0}, γ_I, β_I, Ω_I , δ_I, τ_I	56	-2518.32	5143.73	2.41*
	J_{I0}, $c_{I0} = \Omega_I$, k_{I0}, γ_I, β_I, δ_I, τ_I	48	-2542.86	5181.28	35.35
FI 90	J_{I0}, $c_{I0} = k_{I0}$	8	-34644.27	69304.54	33352.62
	J_{I0}, $c_{I0} = k_{I0}$, $\alpha_I = \beta_I$	24	-26809.98	53668.03	17716.11
	J_{I0}, c_{I0}, k_{I0},	24	-19857.39	39762.86	3810.93
	J_{I0}, c_{I0}, k_{I0}, γ_I	32	-18406.87	36877.87	925.95
	J_{I0}, c_{I0}, k_{I0}, $\alpha_I = \beta_I$	32	-19321.66	38707.45	2755.52
	J_{I0}, c_{I0}, k_{I0}, α_I	32	-19736.85	39537.82	3585.90
	J_{I0}, c_{I0}, k_{I0}, γ_I, $\alpha_I = \beta_I$	40	-18306.65	36693.51	741.59
	J_{I0}, c_{I0}, k_{I0}, γ_I, α_I	40	-18387.14	36854.49	902.57
	J_{I0}, c_{I0}, k_{I0}, α_I, β_I	40	-19313.81	38707.82	2755.90
	J_{I0}, c_{I0}, k_{I0}, γ_I, α_I, β_I	48	-18306.62	36709.53	757.61
	J_{I0}, c_{I0}, k_{I0}, γ_I, α_I, β_I, Ω_I	56	-18182.18	36476.75	524.83
	J_{I0}, c_{I0}, k_{I0}, γ_I, α_I, β_I, Ω_I, δ_I	56	-18209.69	36171.79	219.86
	J_{I0}, c_{I0}, k_{I0}, γ_I, α_I, β_I, Ω_I, δ_I, τ_I	64	-17914.83	35958.18	6.25
	J_{I0}, c_{I0}, k_{I0}, γ_I, β_I, Ω_I , δ_I, τ_I	56	-17919.76	35950.26	0*
	J_{I0}, $c_{I0} = \Omega_I$, k_{I0}, γ_I, β_I, δ_I, τ_I	48	-17931.15	35956.92	6.66

Note. Models are labeled with the free parameters that were allowed to vary. The number of free parameters for each model is equal to the number of free parameters allowed to vary times the number of rats (8). Models were fit to 11447 and 16277 data points for FI 30 and FI 90, respectively. *The constrained model with the fewest free parameters and a ΔAICc < 4 was selected.

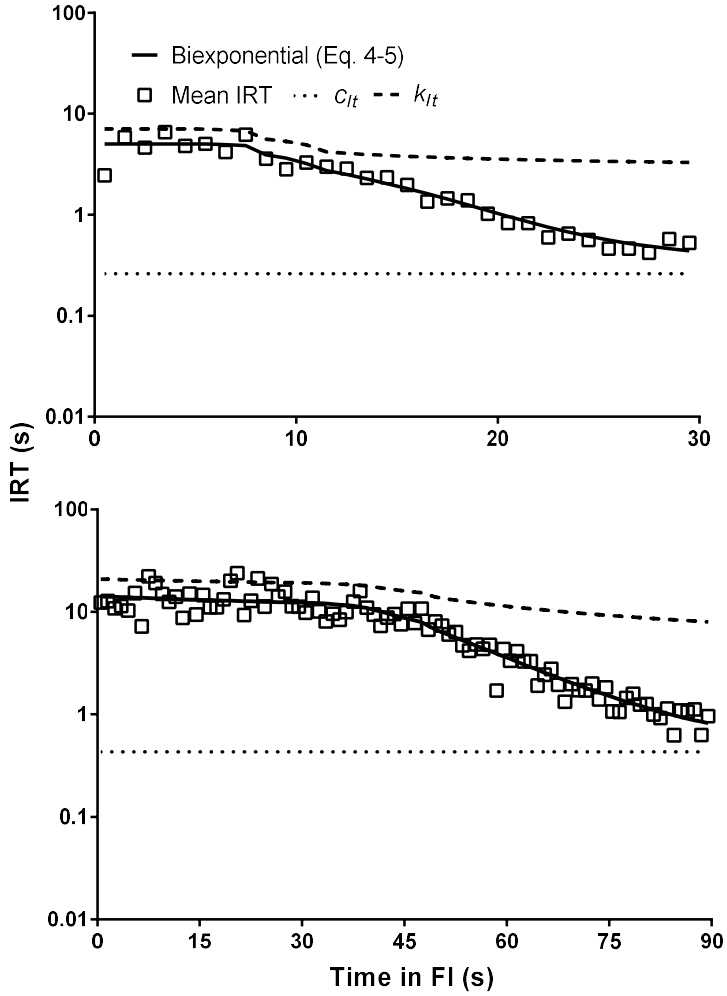

Fig. B2. Left panel: Mean IRT of FI30 and FI 90 rats as a function of time (1-s bins) in the FI. The continuous curve is the mean fit of Eqs. 4 and 5; the dashed curves are mean between-bout (k_{It}) and the dotted curves are the mean within-bout (c_{It}) IRT. Right panels: Note that, in all panels, the y-axis is log base 10 and the x-axis is linear.

APPENDIX C

FIT OF MODELS AND OUTPUT OF SIMULATOR

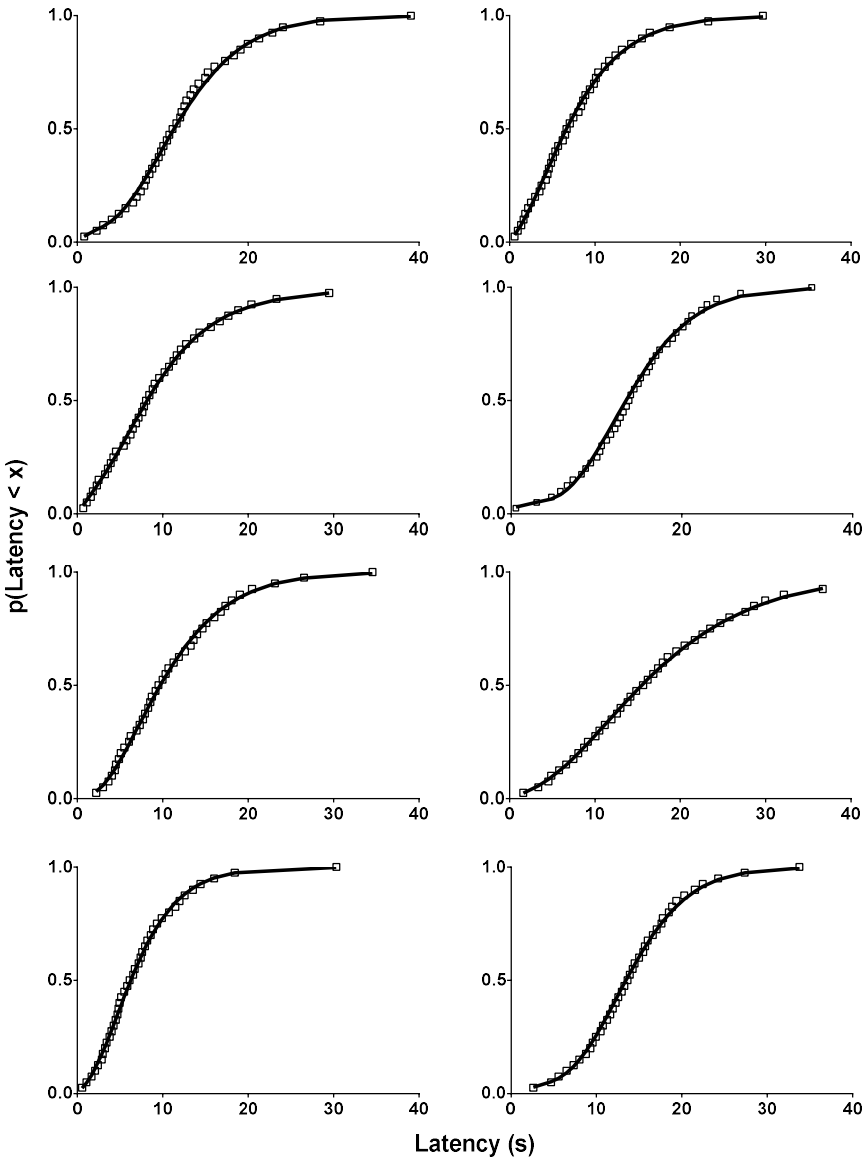

Fig. C1 Empirical cumulative density functions for each rat trained on FI 30-s. Starting on the left side, going down, and then the right and going down rats are numbered 1-8. The solid line trace is the fit of the mixture model described by Eq. 3.

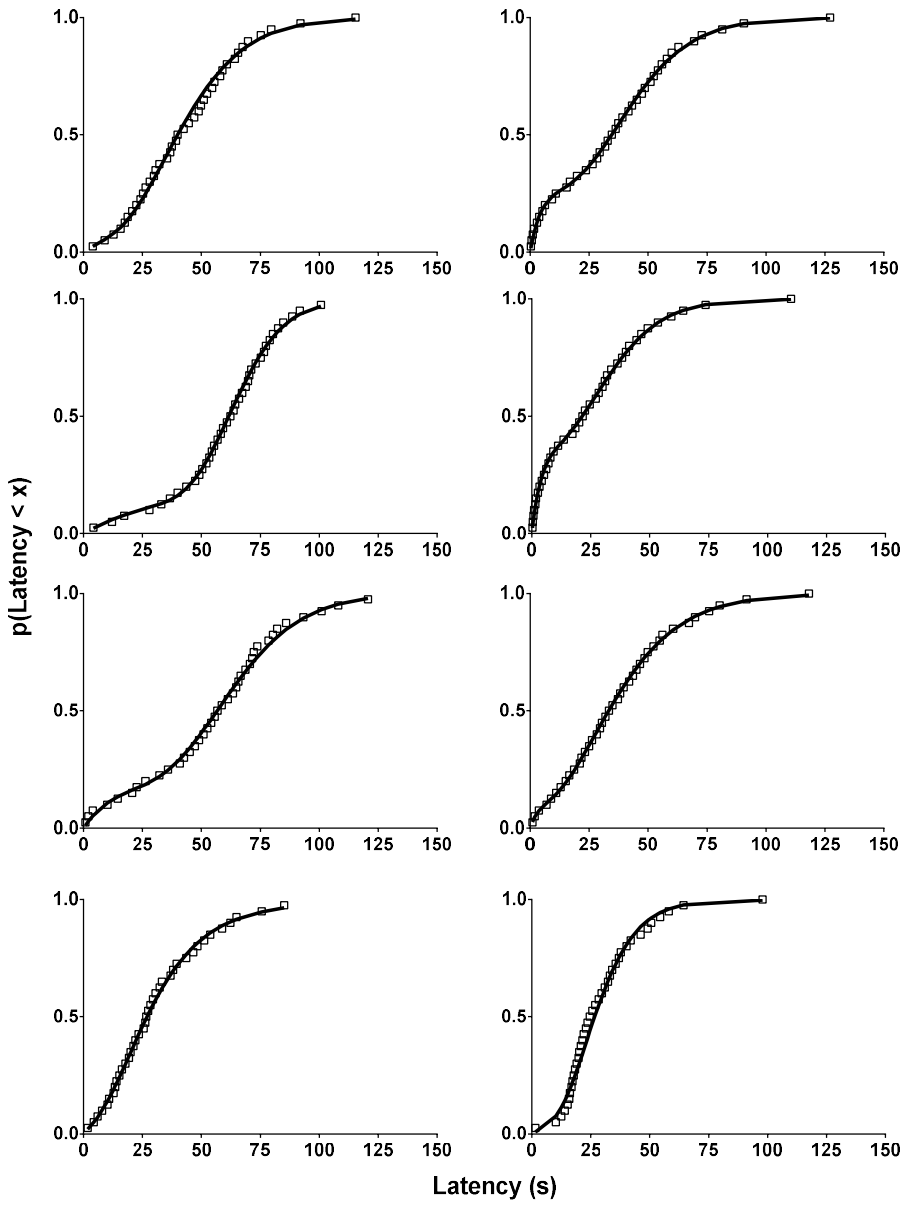

Fig. C2 Empirical cumulative density functions for each rat trained on FI 90-s under the baseline condition. See Fig. C1 for details about organization of the figure and legend.

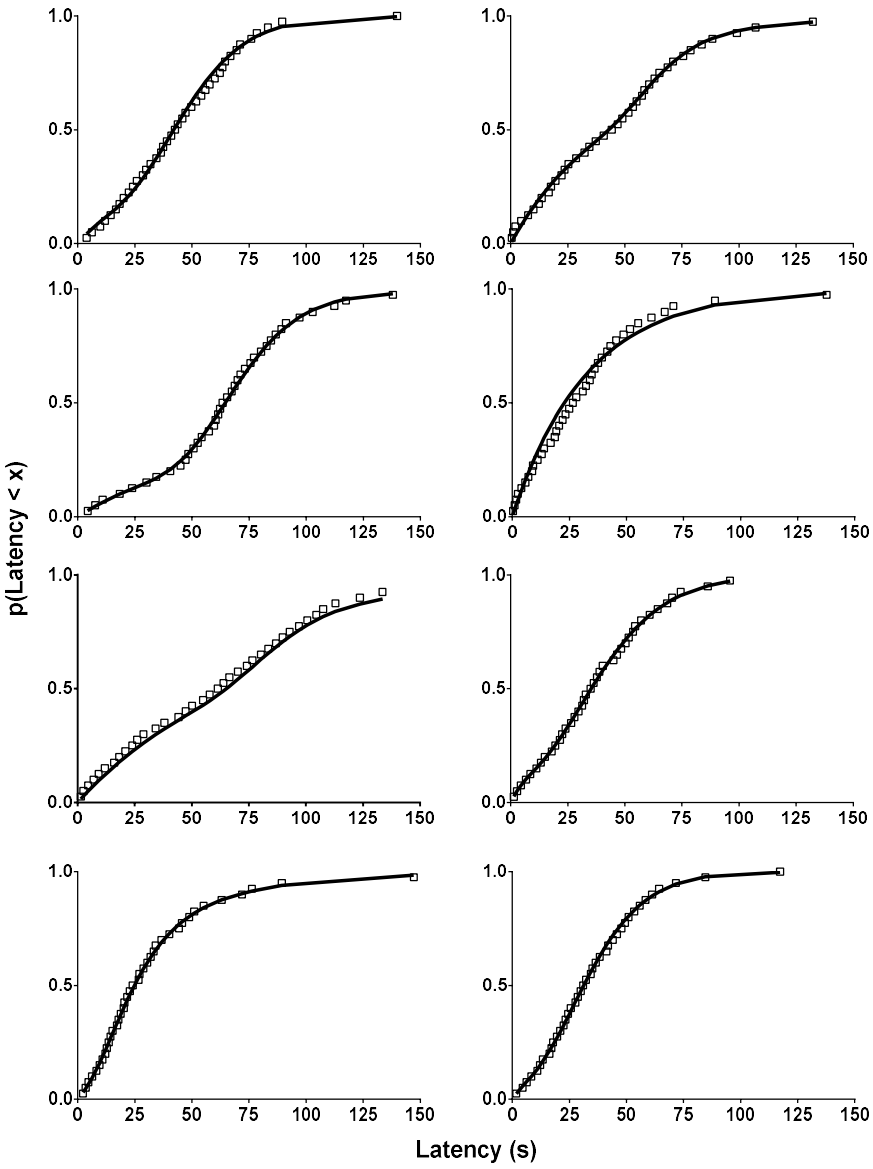

Fig. C3 Empirical cumulative density functions for each rat trained on FI 90-s under the pre-feeding condition. See Fig. C1 for details about organization of the figure and legend.

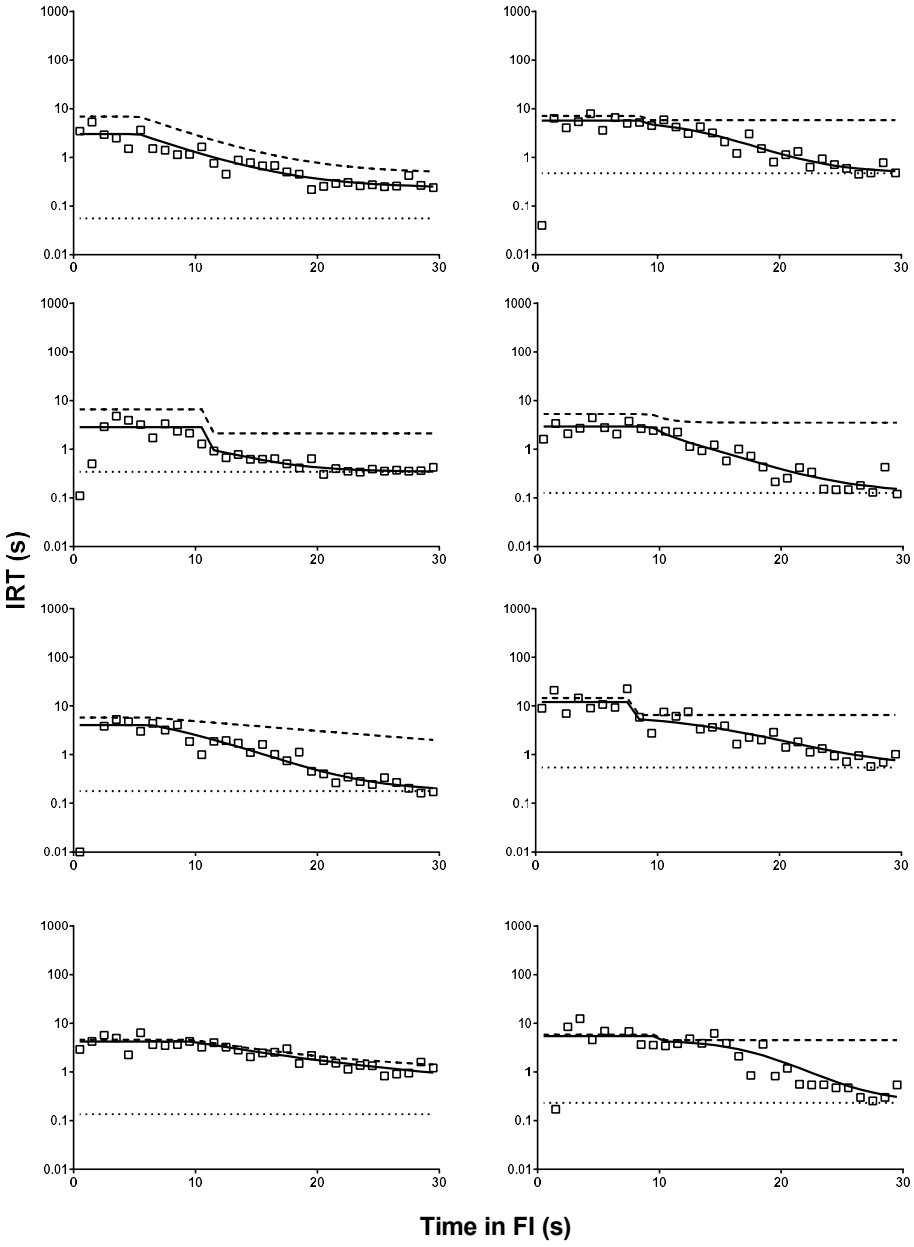

Fig. C4 Mean IRT as a function of time (1-s bins) for each rat trained on FI 30-s. See Fig C1 for details about organization of figure. See Fig. B2 for details about the legend.

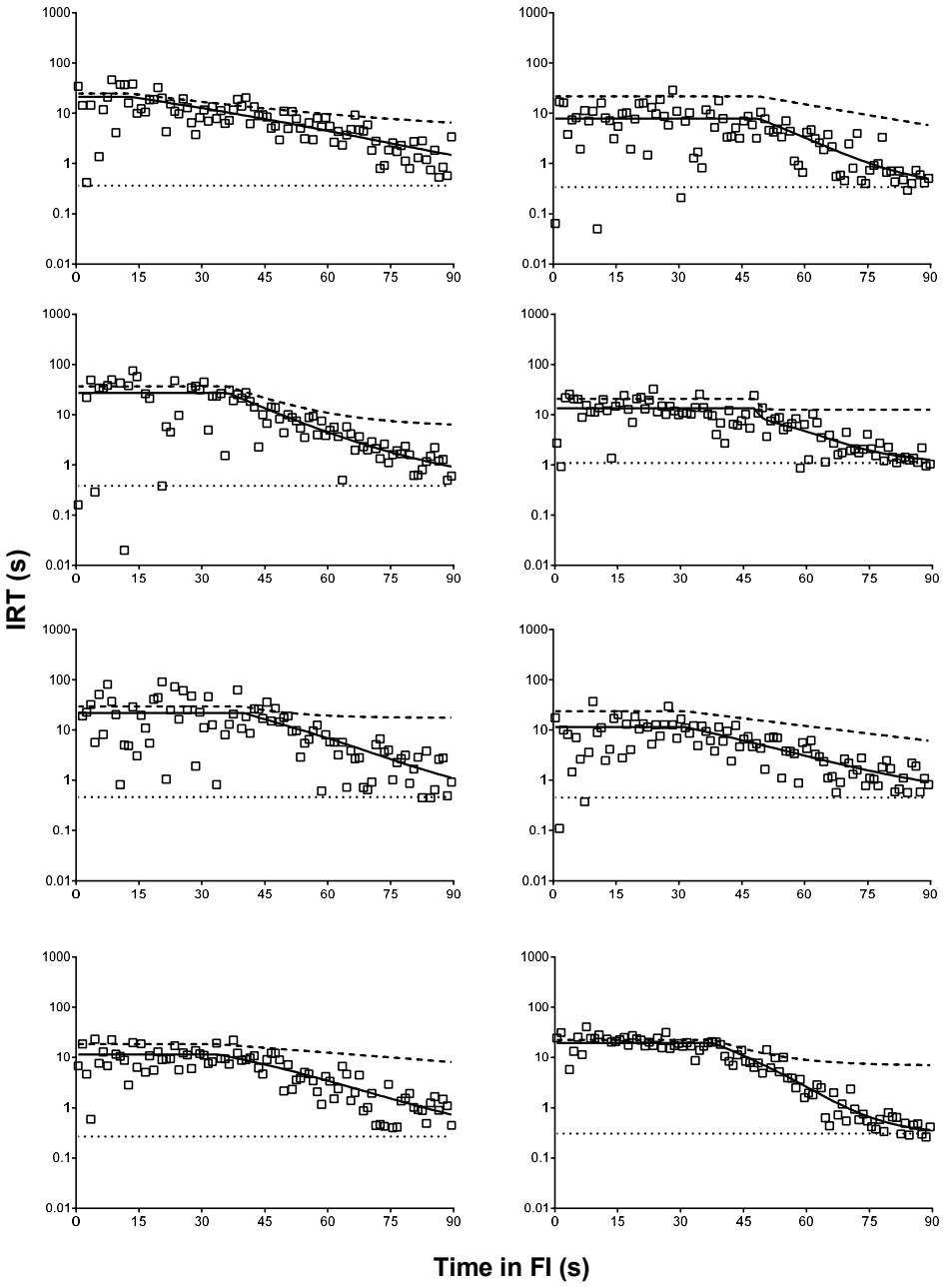

Fig. C5 Mean IRT as a function of time (1-s bins) for each rat trained on FI 90-s. See Fig C1 for details about organization of figure. See Fig. B2 for details about the legend.

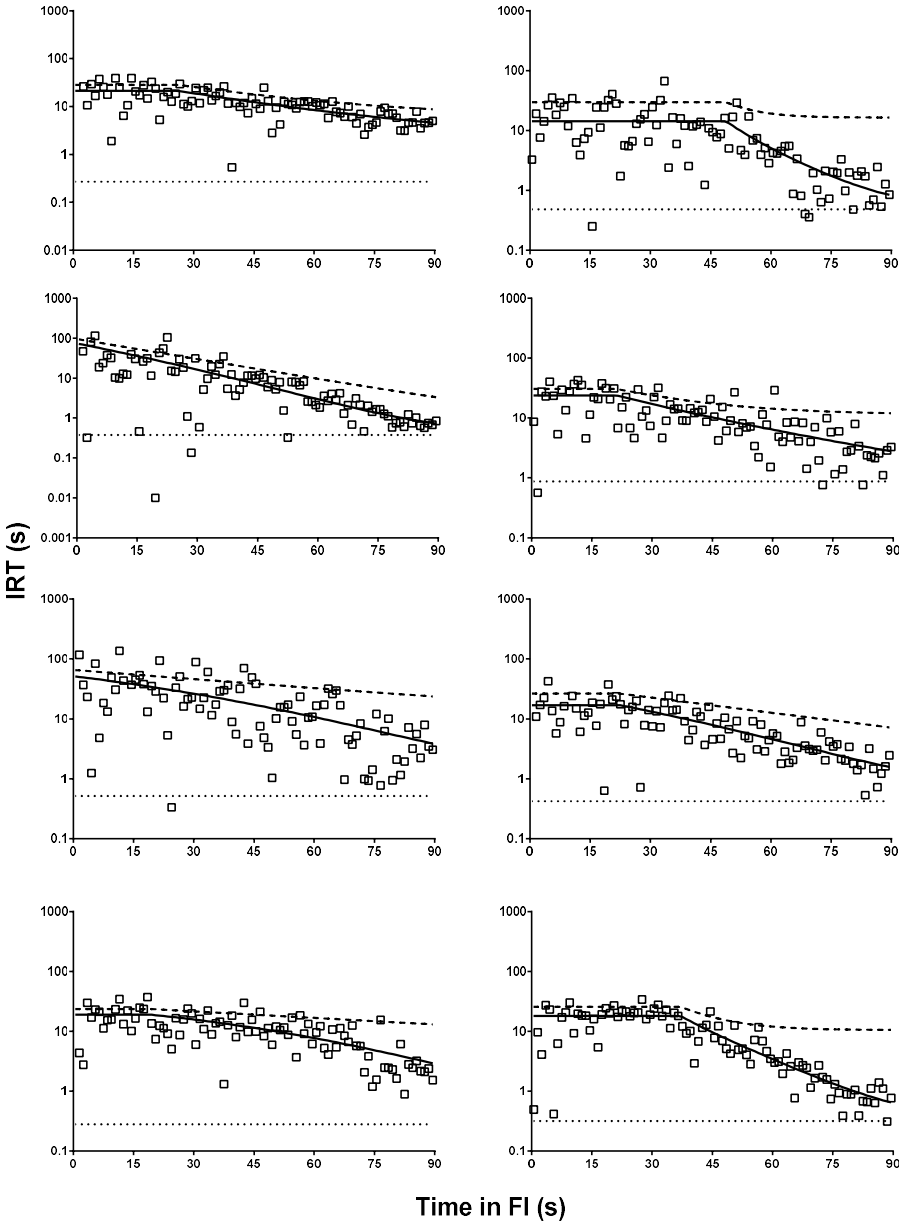

Fig. C6 Mean IRT as a function of time (1-s bins) for each rat trained on FI 90-s under the pre-feeding condition. See Fig C1 for details about organization of figure. See Fig. B2 for details about the legend.

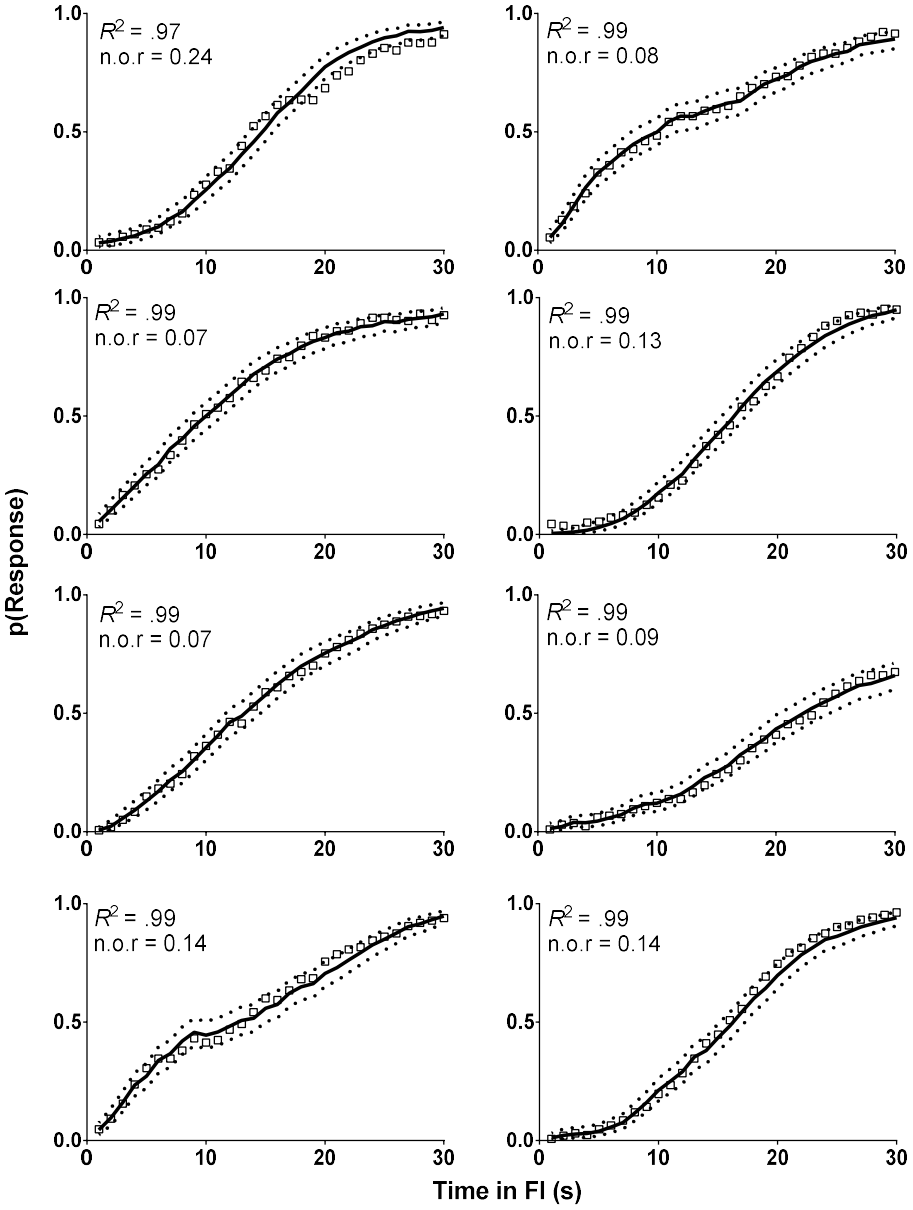

Fig. C7 Mean response functions for each rat trained on FI 30-s as depicted in Fig. 1 plotted against the mean response function (solid line) and ± 2 standard deviations(dashed lines) as predicted by the simulator. See Fig. 1C for details about organization of figure and Fig. 8 for details about the legend.

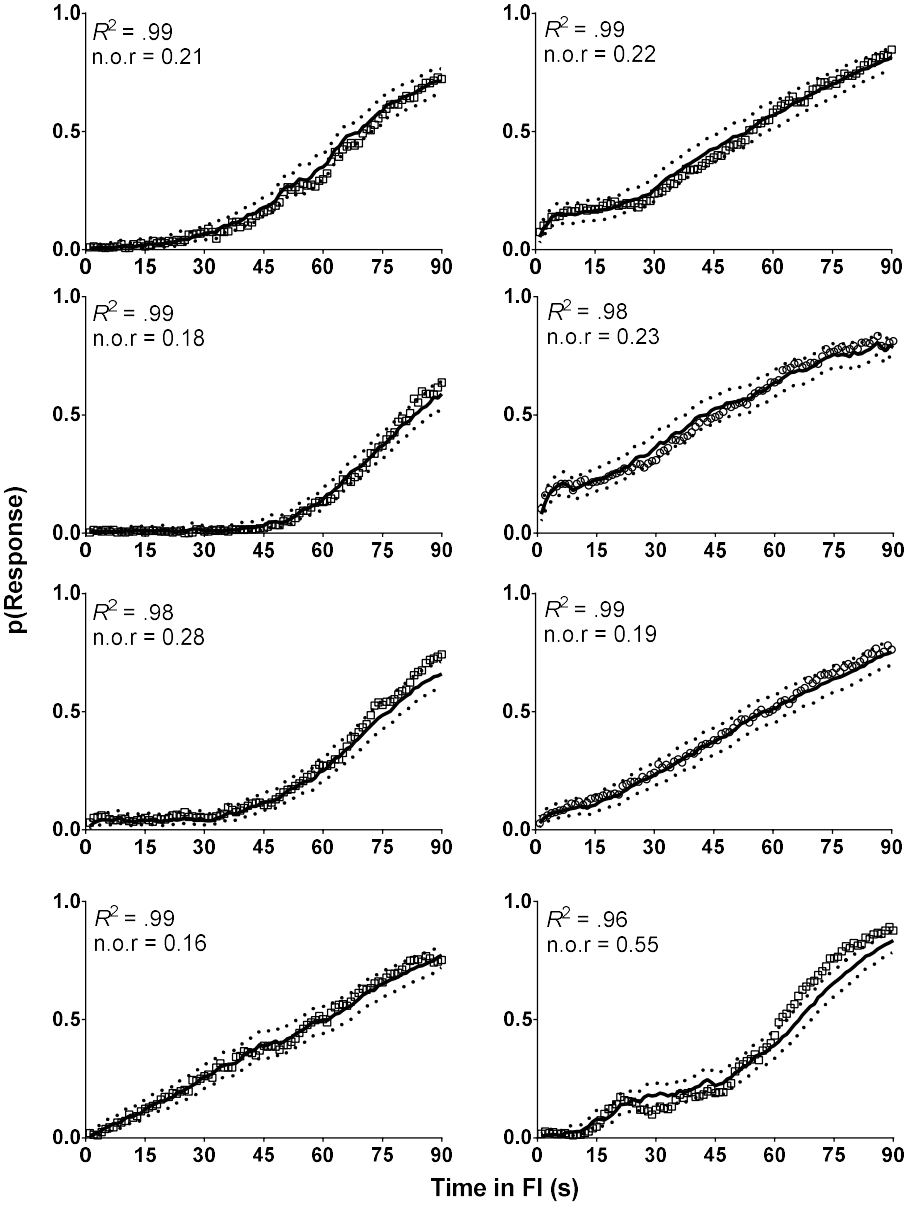

Fig. C8 Mean response functions for each rat trained on FI 90-s under the baseline condition as depicted in Fig. 1 plotted against the mean response function (solid line) and ± 2 standard deviations(dashed lines) as predicted by the simulator. See Fig. 1C for details about organization of figure and Fig. 8 for details about the legend.

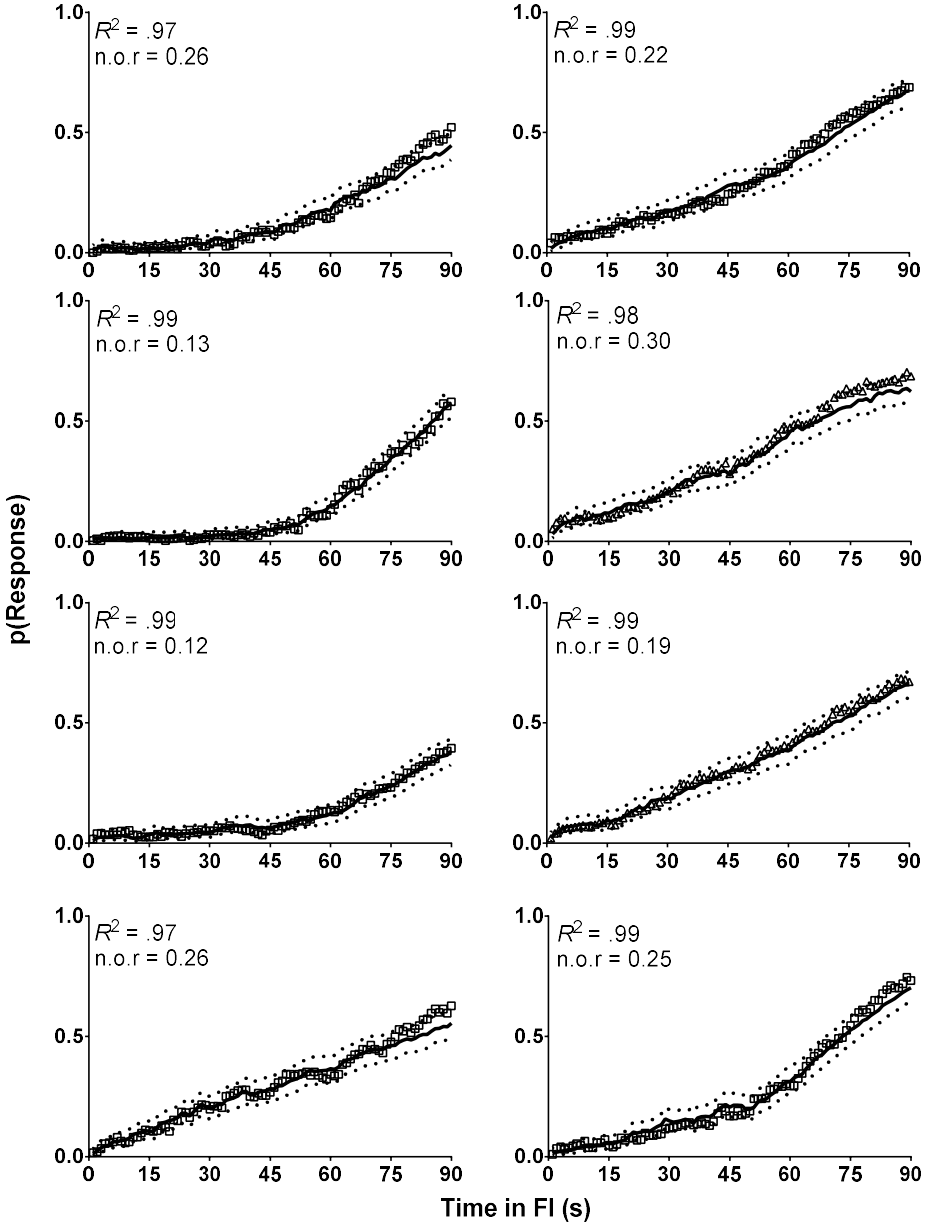

Fig. C9 Mean response functions for each rat trained on FI 90-s under the pre-feeding condition as depicted in Fig. 1 plotted against the mean response function (solid line) and ± 2 standard deviations(dashed lines) as predicted by the simulator. See Fig. 1C for details about organization of figure and Fig. 8 for details about the legend.